

Soft Matter

Accepted Manuscript

This article can be cited before page numbers have been issued, to do this please use: M. F. Thees, J. A. McGuire and C. B. Roth, *Soft Matter*, 2020, DOI: 10.1039/D0SM00565G.



This is an Accepted Manuscript, which has been through the Royal Society of Chemistry peer review process and has been accepted for publication.

Accepted Manuscripts are published online shortly after acceptance, before technical editing, formatting and proof reading. Using this free service, authors can make their results available to the community, in citable form, before we publish the edited article. We will replace this Accepted Manuscript with the edited and formatted Advance Article as soon as it is available.

You can find more information about Accepted Manuscripts in the [Information for Authors](#).

Please note that technical editing may introduce minor changes to the text and/or graphics, which may alter content. The journal's standard [Terms & Conditions](#) and the [Ethical guidelines](#) still apply. In no event shall the Royal Society of Chemistry be held responsible for any errors or omissions in this Accepted Manuscript or any consequences arising from the use of any information it contains.

Review and Reproducibility of Forming Adsorbed Layers From Solvent Washing of Melt Annealed Films

Michael F. Thees, Jennifer A. McGuire, Connie B. Roth*

Department of Physics, Emory University, Atlanta, Georgia, 30322 USA

* E-mail: cbroth@emory.edu

Submitted to *Soft Matter*: January 8, 2020

Revised version submitted March 31, 2020

Recent studies suggest chain adsorption in the melt may be responsible for a number of property changes in thin films by making correlations between the residual adsorbed layer thickness $h_{\text{ads}}(t)$ measured after a given solvent washing procedure as a function of annealing time t of the film at an elevated temperature prior to this solvent rinse. This procedure, frequently called “Guiselin’s experiment”, refers to the thought experiment proposed in a 1992 theoretical treatment by Guiselin that assumed chain segments in contact with the surface are irreversibly adsorbed whereby unadsorbed chains could be washed away by solvent without disturbing the adsorbed substrate contact points in the melt. In the present work, we review this recent literature, identifying and experimentally testing a common protocol for forming adsorbed layers $h_{\text{ads}}(t)$ from solvent washing melt films. We find $h_{\text{ads}}(t)$ curves to be far less reproducible and reliable than implied in the literature, strongly dependent on solvent washing and substrate cleaning conditions, and annealing at elevated temperatures is unnecessary as densification of films sitting at room temperature makes the glassy film harder to wash off, leaving behind h_{ads} of comparable thickness. This review also summarizes literature understanding developed over several decades of study on polymer adsorption in solution, which experimentally demonstrated that polymer chains in solution are highly mobile, diffusing and exchanging on the surface even in the limit of strong adsorption, contradicting Guiselin’s assumption. Preformed adsorbed layers of different thicknesses h_{ads} are shown to not affect the average glass transition temperature or physical aging of 30 nm thick films. In summary, a number of open questions and implications are discussed related to thin films and polymer nanocomposites.

1 Introduction

In recent years a few groups have suggested that adsorption of chains to substrate interfaces occurs in melt films acting to modify the anomalous dynamics observed in ultrathin films and other ‘nanoconfined’ systems. These reports typically correlate some observed change in dynamics after prolonged annealing at an elevated temperature with parallel measurements of the thickness of a residual layer after a given solvent washing protocol on films that have been nominally annealed under equivalent conditions.^{1–13} This residual adsorbed layer thickness $h_{\text{ads}}(t)$ as a function of annealing time at elevated temperature is frequently reported under the assumption that the solvent washing procedure used “reveals” the adsorbed layer structure formed in the melt (termed “Guiselin’s experiment” or approach).^{1,6,10,14–20} Thicker residual layers after solvent washing are found for films that have been annealed longer, from which authors have concluded that adsorbed layers are responsible for perturbations to the glass transition temperature $T_g(h)$ in thin films,^{1,6,8,21,22} increased viscosity of thin films,^{2,9} as well as other anomalous property changes observed in thin films spanning deviations to density,²³ thermal expansion,¹⁶ dewetting,^{5,20} crystallization,^{10,24} and water uptake.²⁵ Given the prevalence of observations being attributed to chain adsorption in melt films, we believe it is imperative that the reliability and reproducibility of the experimental method used to ascertain such conclusions is evaluated.

In this work, we summarize this recent literature comparing the various results reported for the residual adsorbed layer thickness $h_{\text{ads}}(t)$ measured after solvent washing as a function of annealing time at 150 °C for polystyrene (PS) films on piranha cleaned silicon wafers, the most commonly reported case. We attempt to distill and test a coherent common protocol for the formation of adsorbed layers used in these various studies. In particular, we evaluate the impact of substrate cleaning method, solvent washing procedure used, ellipsometry measurement precision, and various other experimental protocol details on the reproducibility and reliability of forming adsorbed layers. We discuss these results in the context of the older, well-established 1950s–1990s literature on polymer adsorption in solution, and the two and a half decades of literature on anomalous dynamics in nanoconfined thin films. Our primary focus is to address the reliability and understanding associated with forming adsorbed layers $h_{\text{ads}}(t)$ from the melt, from which inferences have been made about the importance of chain adsorption for modifying dynamics in thin films. We do not review or evaluate the reported changes in dynamics attributed to adsorption themselves, which is beyond the scope of the present work.

1.1 Summary of Recent Investigations on Adsorbed Layers Formed from Melt Films

The recent reports in the literature that claim to correlate large changes in dynamics with the presence of an adsorbed layer utilize, in general, a common experimental protocol for obtaining adsorbed layers from melt films, but vary widely in the details of exactly how each step is performed. According to these studies, the basic procedure for creating an adsorbed layer involves cleaning the substrate, spin-coating a (typically bulk) polymer film on top, annealing the film at an elevated temperature for some extended length of time t , and then using a good solvent to wash away “unadsorbed chains”.^{4,14,15,22,26,27} The remaining residual adsorbed layer thickness $h_{\text{ads}}(t)$ left behind on the substrate after the solvent washing procedure is then measured, most often by ellipsometry.^{1,14,17–19,22,26,27} Although frequently not explicitly stated, the refractive index parameters for these ellipsometry measurements are typically held constant at the bulk value,^{16,18} because these films are very thin, frequently less than 10 nm, and ellipsometry has difficulty independently resolving thickness and refractive index for such thin films.^{28,29} A couple of groups have also used atomic force microscopy (AFM) to confirm the h_{ads} values measured by ellipsometry match those obtained from a step-height measurement.^{14,27}

In studies of chain adsorption from the melt, silicon substrate cleaning has most frequently been done with piranha solution (7:3 $\text{H}_2\text{SO}_4:\text{H}_2\text{O}_2$),^{4,19,22,27} which strongly oxidizes organics allowing them to be rinsed away by water, leaving a highly hydrophilic SiO_x surface. Other studies have used a hydrogen fluoride (HF) treatment of silicon substrates, which strips the native oxide layer, and usually shows higher amounts of chain adsorption.^{26,27} Alternately, some groups use a progressive series of organic solvents to clean substrates.^{14,15,30} After cleaning, bulk polymer films are spin-coated onto the substrates, and the samples are then annealed at an elevated temperature, usually under vacuum^{4,19,22,26} or in some works on a hot plate.^{15,18,24,27} This annealing step is thought to facilitate the growth of the adsorbed layer as the measured residual thickness $h_{\text{ads}}(t)$ is found to increase with increasing annealing time t .^{1,4,5,7,14,17–19,22,26,30} A solvent washing procedure where the annealed films are immersed in a good solvent for some prolonged time, in some cases multiple times, is then used to “reveal” the adsorbed layer that was presumed to have formed in the melt.^{4,14,15,20,26,30} Most frequently the solvent is that used for spin coating the initial film (e.g., toluene),^{14,15,22,26,27} although occasionally a stronger solvent like chloroform is used instead.^{4,16,20}

This solvent washing step varies widely in the literature both in the length of time a film is washed and in the total number of washes conducted. As we will demonstrate that solvent washing is a defining step in the resulting $h_{\text{ads}}(t)$ measured, we summarize here the various washing procedures used by the existing studies. Napolitano et al. and Koga et al., two groups who have made significant claims in the recent literature on polymer adsorption from the melt, have developed similar, but distinctly different protocols for washing off unadsorbed chains. Napolitano et al. frequently report changes in film properties as a function

of annealing time that are then correlated with separate measurements of the adsorbed layer thickness.^{1,3,7,8,12} For these experiments, they report using one 30 min wash in toluene¹⁴ or one 30 min wash in chloroform¹⁶ to remove the unadsorbed chains. However, several studies do not report details for their washing protocol, with some stating simply that “non-adsorbed chains were washed away in the same good solvent used for spin-coating (toluene)”,¹ or instead refer to a previous publications for experimental details.^{7,15,17,18} In contrast, Koga et al. report the most extensive and detailed washing procedure believing that extended solvent washing further reveals different structures of the adsorbed layer in the melt. An initial series of washes, 3–5 times 30 min in toluene,^{19,20,26} is used to expose the “interfacial sublayer”.^{4,19,20} The more loosely bound chains can then also be removed by a “further prolonged leaching process (up to 150 days)” in toluene, exposing the more tightly bound “lone flattened higher density layer”.²⁶ More recent works have replaced the 150 days in toluene with only “a couple of days” in a stronger solvent, chloroform,⁴ or more recently three times 30 min in chloroform.²⁰ Other groups have used three 10-minute washes in toluene to obtain the residual adsorbed layer.^{22,27}

Given the large differences in experimental protocol for producing residual adsorbed layer thicknesses, we directly compare in Figure 1 reported literature data for $h_{\text{ads}}(t)$ as a function of annealing time t at an elevated temperature above T_g from a number of different studies.^{4,14,22,26,27} For this comparison, we primarily chose $h_{\text{ads}}(t)$ data representing what appears to be the most common experimental protocol, PS films on piranha cleaned silicon substrates annealed at 150 °C under vacuum^{4,5,19,20,22} or in air.²⁷ We also include the closest comparable data from Napolitano’s group of PS films on solvent cleaned silicon substrates annealed at 140 °C on a hot plate.¹⁴ Solvent washing of these PS films were all done in toluene under roughly comparable conditions: three 10-min washes,^{22,27} one 30 min wash,¹⁴ or 5+ (likely 10-min) washes.⁴ As shown in Figure 1a, the trends in $h_{\text{ads}}(t)$ typically show an initial rapid increase in h_{ads} that saturates at some long-time plateau $h_{\text{ads}}(t = \infty) = h_{\infty}$ after a few hours (5–10 h) of annealing,^{4,22,26,27} with larger h_{∞} values being observed at higher molecular weights.^{26,27} The $h_{\text{ads}}(t)$ data are most simply fit to a function having the general form of

$$h_{\text{ads}}(t) = h_{\infty}(1 - e^{-t/\tau}) \quad (1)$$

to determine the final long-time plateau h_{∞} value, where τ represents some characteristic time.

The study from Tsui et al. provided only final long-time plateau h_{∞} residual thickness values for a range of molecular weights spanning from $M_w = 13.7$ to 940 kg/mol,²⁷ plotted to the far right side of the graph in Fig. 1a. They demonstrated that these h_{∞} values scaled linearly with the radius of gyration R_g ($h_{\infty} = 0.47R_g$) as plotted in Figure 1b, where it was assumed that $R_g \sim N^{1/2}$ for melts.²⁷ Similar data collected on HF treated silicon showed larger h_{∞} values also scaling with R_g , $h_{\infty} = 0.81R_g$.²⁷ These data, as well as complementary data by Koga et al.²⁶ are also plotted in Figure 1b. This scaling of the long-time plateau h_{∞} residual thickness with the radius of gyration R_g of the chain was previously

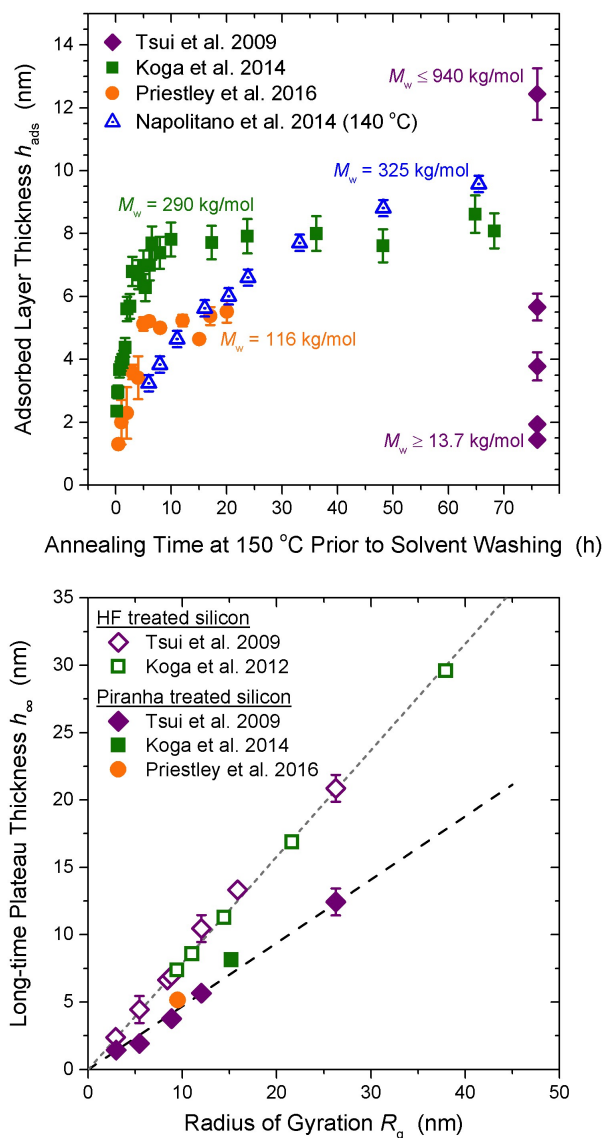


Fig. 1 (a) Comparison of literature data for the residual adsorbed layer thickness $h_{\text{ads}}(t)$ remaining after solvent washing with toluene as a function of annealing time at 150 °C for PS films on piranha cleaned silicon wafers: data from Tsui et al.²⁷ (purple diamonds at long annealing times for a range of molecular weights $M_w = 13.7 - 940$ kg/mol) and Priestley et al.²² (orange circles, $M_w = 116$ kg/mol) are for three 10 min washes, while that from Koga et al.⁴ (green squares, $M_w = 290$ kg/mol) are for three 30 min washes. Data from Napolitano et al. (blue triangles, $M_w = 325$ kg/mol) at 140 °C, the closest comparable temperature, are also included, where samples were washed once for 30 min.¹⁴ (b) Final residual thickness plateau h_{∞} obtained at long annealing times on both piranha cleaned silicon (closed symbols) and HF treated silicon (open symbols) plotted as a function of radius of gyration, assuming $R_g \sim N^{1/2}$. Data are replotted from Tsui et al.,²⁷ with additional data from Koga et al.²⁶ and estimated from Priestley et al.²² and Koga et al.'s 2014 study.⁴

demonstrated by Durning et al.,³¹ who appear to be the first to investigate the formation of residual polymer layers formed from solvent washed melt films. In their study 1 μm thick poly(methyl methacrylate) (PMMA) films were annealed at 165 °C for up to 120 h in an argon atmosphere on quartz substrates that were ini-

tially cleaned with a hydrochloric acid (HCl) based treatment. The annealed films were then washed three times for 3 h in benzene, the spin-coating solvent, followed by sonicating for 5-10 min, prior to measuring the dry residual layer thickness remaining (i.e., h_{ads}) with neutron reflectivity. Films were made from a range of molecular weights, $M_n = 13 - 1230$ kg/mol, with the final adsorbed layer thickness reached at long times scaling as $h_{\infty} \sim N^{0.47 \pm 0.5}$.

The $h_{\text{ads}}(t)$ data shown in Fig. 1a from Napolitano's group are for an annealing temperature of 140 °C. This study by Housmans et al. compared $M_w = 325$ kg/mol at three different annealing temperatures (140, 170, and 180 °C) finding that $h_{\text{ads}}(t)$ increases faster with increasing temperature.¹⁴ Data for $M_w = 1460$ kg/mol at 140 °C showed that $h_{\text{ads}}(t)$ also increases faster for higher molecular weights. Not enough data is provided to estimate the final adsorbed amount h_{∞} at long times, but as the data can be collapsed by scaling only the time axis, it appears that the final adsorbed amount would be independent of temperature. Koga et al. has also shown that h_{∞} is independent of annealing temperature from 40-150 °C.²⁶ Napolitano et al. fit the slower growth of $h_{\text{ads}}(t)$ they observe to a two-stage functional form:

$$h_{\text{ads}}(t) = \begin{cases} h_0 + \nu t, & t < t_{\text{cross}} \\ h_{\text{cross}} + \Pi \log(t/t_{\text{cross}}), & t > t_{\text{cross}} \end{cases} \quad (2)$$

where h_0 is the initial adsorbed amount at $t = 0$, while t_{cross} and h_{cross} identify a transition point between a linear and logarithmic regime with respective growth rates ν and Π .^{14,15,30}

This basic protocol of annealing and then solvent washing films as a method of obtaining adsorbed layers has been frequently referred to as following "Guiselin's experiment"^{1,6,14-18} or "Guiselin's approach",^{10,19,20} citing the 1992 study by O. Guiselin.³² This Guiselin work is a theoretical treatment using scaling analysis to determine the concentration profile of adsorbed chains in contact with a surface.³² In particular, Guiselin proposes the thought experiment of starting with an equilibrated melt film in contact with a surface that is then washed with solvent to leave behind an adsorbed layer. In the theoretical treatment, Guiselin makes two critical assumptions:³² (i) that the melt chains initially in contact with the substrate surface have an equilibrated Gaussian distribution, which is used to define the set of chain segments in contact with the surface, and (ii) that these contact points are then "irreversible" such that each polymer segment-surface contact remains permanently bound during the solvent washing step where all unadsorbed chains are removed. It is this thought experiment that drives the experimental procedure and interpretation of results described above, where the extended annealing time at elevated temperatures prior to solvent washing is thought to be required to reach the equilibrated melt state envisioned by Guiselin and that the solvent washing procedure merely "reveals" the structure of the adsorbed layer that was formed during this melt state annealing.^{1,4,14,15,19,21,26,30}

In the remainder of this work we address whether or not this interpretation is correct: first by summarizing the extensive body of literature and understanding that was developed from the study of polymer adsorption in solution, then second by experimentally

evaluating the reproducibility and reliability of forming $h_{\text{ads}}(t)$ curves as shown in Figure 1. As we cannot possibly evaluate all permutations of the experimental protocols used in the literature, we instead investigate the most common procedure used and address the impact of varying what we believe are the most key factors. Figure 2 outlines the basic set of experimental steps we will follow and evaluate for producing and measuring adsorbed layers formed from solvent washing melt annealed films. Silicon wafer substrates with a native oxide layers will be rigorously cleaned with piranha solution, or later with an HCl solution found to produce equivalent results. Other common substrate cleaning methods using organic solvents will also be addressed. Bulk films with thicknesses $h > 200$ nm of PS ($M_w = 400$ kg/mol) will be spin-coated onto the freshly cleaned substrates and then annealed above T_g under vacuum for some period of time t , most typically at 150 °C for up to 60 hours. These samples will then be washed in toluene, a good solvent, most commonly for a single 30 min wash; however, we will also explore the impact of multiple solvent washes. The final dried films remaining after the solvent washing procedure will be measured using spectroscopic ellipsometry to determine the residual adsorbed layer thickness $h_{\text{ads}}(t)$. As the evaluation of all steps will rely on the accuracy of measuring the thickness of these very thin $h_{\text{ads}}(t)$ layers, typically less than ~ 10 nm, we will start by addressing the reliability of the spectroscopic ellipsometry measurement and the data analysis of fitting to the common optical layer model of a Cauchy layer with a fixed refractive index.

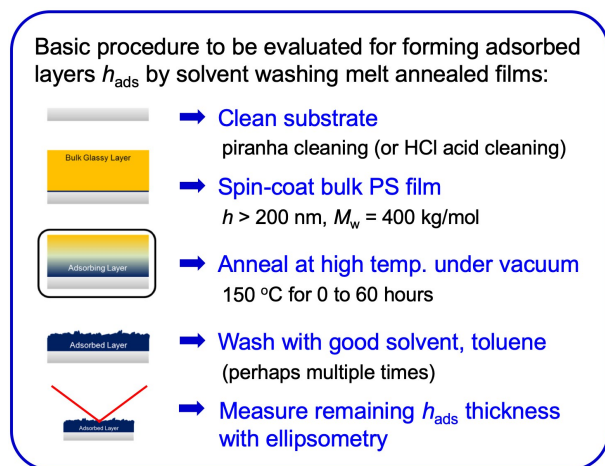


Fig. 2 Illustration of the basic experimental steps to be evaluated for forming adsorbed layers $h_{\text{ads}}(t)$ by solvent washing films that were annealed at an elevated temperature for some length of time t .

1.2 Summary of the Understanding Developed of Chain Adsorption in Solution

The study of polymer adsorption has a long history with investigations dating back to the 1950s.³³ A great deal of work in the field was done from the 1970s-1990s, with major advances occurring in the experimental characterization and theoretical description of polymer adsorption in solution, culminating in the seminal 1993 book by Fleer, Cohen Stuart, Scheutjens, Cosgrove, and Vin-

cent.³⁴ There are also several excellent reviews by de Gennes,³⁵ Cohen Stuart and Fleer,^{36,37} Granick,^{38,39} Douglas et al.,⁴⁰ and an excellent pedagogical chapter in Jones and Richards book, *Polymer Surfaces and Interfaces*.⁴¹ These early efforts on chains in solution set the stage for studies on protein adsorption where additional electrostatic interactions need to be incorporated to account for charges on both the chain and in solution.^{42,43} Surface science textbooks^{44,45} also describe numerous types of adsorption behavior for a range of different systems, with extensive work on gases demonstrating complex isotherms depending on neighboring interactions and other factors, having long since expanded beyond the original simple Langmuir adsorption model.⁴⁶ In contrast, adsorption isotherms for polymers are usually so steep that there is little ability to characterize features. In the present review, we focus on summarizing the understanding developed for polymer adsorption in solution that would be relevant to interpreting the experimental studies of polymer adsorption in melts. Most of this comes from the earlier literature on uncharged systems.

The basic adsorption mechanism results from a favorable energy gain for polymer segments to be in contact with the surface over a solvent molecule. This is despite an entropic conformational energy penalty for partially unfolding the chain to make these polymer segment-surface contacts. There is also translational entropy lost by an adsorbed species in contact with the surface where larger molecules can make more surface contacts per molecule for the same translational entropy loss. However this is not the primary reason why high molecular weight chains adsorb preferentially in solution; instead, the main driving force comes from the strongly reduced entropy of mixing for large chains in solution.³⁴ Overall it is the free energy balance of the entire system that makes it entropically more advantageous to have small solvent molecules free in solution with larger polymer chains at the surface, unless there is a much stronger favorable interaction between the solvent molecule and the surface.

There have been numerous theoretical approaches over the years for treating polymer adsorption to surfaces.^{34,41} The main approaches have been a self-consistent mean field theory (SCFT) treatment extensively developed by Scheutjens and Fleer,^{47,48} based on a lattice theory similar to the standard Flory-Huggins formulation for blends, and a scaling theory formulation with an initial treatment by de Gennes⁴⁹ and then subsequent work by Guiselin and Aubouy.^{32,50} The scaling approach is considered better for diffuse adsorbed layers found in dilute solutions, technically only rigorously valid in the limit of long chains at very low solution concentrations.^{35,41} The concern with mean-field treatments like SCFT is that they tend to only work well for systems with weak fluctuations as in concentrated solutions and melts. However, as polymer concentration within the adsorbed layer near the surface is usually high this may be less of a concern; mean field treatments also have the advantage of being readily adaptable computationally.⁴¹

Initially developed to explain classic adsorption experiments in solution, these models provide statistical descriptions of adsorption isotherms and segment density distributions as a function of distance from the surface for adsorbed layers in equilibrium.

Chain conformations of surface attached chains are typically characterized in terms of trains, loops, and tails; terminology dating back to Jenkel and Rumbach in 1951.³³ The loop-train-tail model classifies segments of an adsorbed chain as being part of either a *train*, series of segments in direct contact with the surface, a *loop*, set of segments tethered between two adsorption points, or a *tail*, chain ends dangling into the solution (see depiction in Figure 3a). The classic adsorption experiments in solution characterized the amount of polymer adsorbed to a surface in the equilibrium limit for solutions of different concentration.^{33,34} Figure 3b depicts the typical shape of such an adsorption isotherm where the axes usually correspond to the adsorbed amount Γ as a function of bulk solution concentration c . The thickness of the resulting adsorbed layer has been experimentally found to scale with chain length as $\sim N^{0.4-0.8}$,³⁴ depending on solvent quality and the extent to which the chains stretch out into solution. For a dried film where all solvent has been removed, the resulting adsorbed layer thickness would be expected to scale as $h_{\text{ads}} \sim N^{0.5}$, as was shown in Fig. 1b. The adsorbed amount Γ (mass per unit area) can be determined for a dry film from its residual thickness h_{ads} based on $\Gamma = \rho h_{\text{ads}}$, where bulk density is usually assumed for ρ .^{18,51,52} One can also calculate an effective number density of chains per unit area σ_{ads} by dividing Γ by the mass of a single chain leading to $\sigma_{\text{ads}} = \rho N_A h_{\text{ads}} / M_n$, equivalent to the standard formula used for grafted chains.⁴¹

The key parameter that underpins essentially all theoretical formulations of polymer adsorption to interfaces is the adsorption energy parameter χ_s , often thought of as a segmental “sticking” energy for a given polymer segment to the substrate surface. Although often obscurely or abstractly defined, almost all studies cite the original definition formulated by Silberberg in 1968:⁵³

$$\chi_s = -(u_s - u_s^0) / kT, \quad (3)$$

where u_s and u_s^0 are the interaction energies for a polymer segment–surface contact and a solvent–surface contact, respectively. Eq. 3 expresses χ_s in terms of the thermal energy kT to make it unitless, similar to how the Flory-Huggins interaction parameter is defined. For polymer solution studies, the thermal energy reference temperature was almost always room temperature, and used simply to define the energy scale, where “weak adsorption” was considered to mean χ_s is comparable to kT , while “strong adsorption” implied χ_s is several times kT .⁴⁹ Granick pointed out in his 2002 Perspective³⁹ that this customary definition “implies that it [χ_s] scales with temperature, which is unlikely; it is a misleading convention, because these values are usually determined near room temperature.” In fact, the equilibrium adsorbed amount Γ is observed to decrease with increasing temperature as more thermal energy is available to overcome the likely temperature-independent χ_s adsorption energy, as was shown by Granick et al. measuring at 35 °C only 40% of the surface coverage present at 25 °C.⁵⁴

The second issue with the χ_s definition that is frequently obscured is that the adsorption energy parameter χ_s corresponds to the *difference* in free energy to transfer a polymer segment from the bulk to the surface relative to transferring a solvent molecule

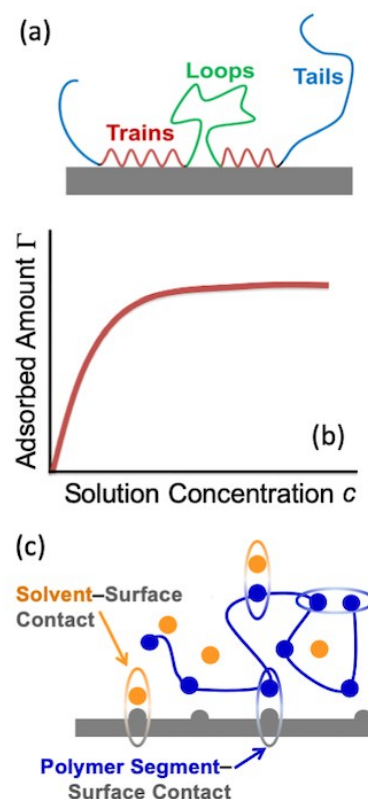


Fig. 3 (a) Cartoon of an adsorbed chain depicting trains, loops, and tails. (b) Schematic of a classic adsorption isotherm in solution, equilibrium adsorbed amount Γ as a function of solution concentration c . (c) Diagram illustrating the different interaction energies in the system, where the segmental “sticking” energy χ_s , eq. 3, is defined as the difference in interaction energy between a polymer segment–surface contact and solvent–surface contact.

from the surface to the bulk (see depiction in Figure 3c). In eq. 3, this exchange of surface contacts is written as the difference ($u_s - u_s^0$) in interaction energy between a polymer segment–surface contact u_s and a solvent–surface contact u_s^0 , with a positive χ_s corresponding to preferential adsorption of polymer segments.^{36,47,53,55} The meaning of this exchange energy is especially unclear when some texts simply define some abstract interaction parameter (e.g., δkT) to represent the “sticking” energy of the polymer chain to the substrate surface,^{49,56} frequently citing the original Silberberg paper⁵³ in the process.

Reference to theoretical works of polymer adsorption in solution that are formulated based on Silberberg’s definition for the adsorption energy parameter χ_s is often cited to justify adsorption in melts,^{4,5,26} even though no solvent is present in the system. Alternatively, others just assume some favorable polymer segment–surface interaction energy of $\sim kT$ without justification for there even being attractive interactions.^{17,30} However, by Silberberg’s definition for χ_s (eq. 3), the adsorption energy parameter χ_s for melts with no solvent would be strictly zero as the difference in free energy would be to exchange one polymer segment–surface contact with another equivalent polymer segment–surface contact. A more proper definition of some “sticking” energy parameter χ_s for a melt system would likely bench-

mark the difference in interaction energy between a polymer segment–surface contact u_s with a polymer segment–segment contact in the bulk u_b^0 , although the theoretical framework would need to be revised because this does not correspond to an equivalent definition in the way eq. 3 is used. We also note that the main driving force for polymer segregation to surfaces in solution, the reduced miscibility of large chains in solution,³⁴ would not be applicable in melts. Leaving only this, likely weak, “sticking” energy to drive adsorption in melts against the entropy cost of unfolding the chain near the surface. Thus, unless there is some strongly favorable interaction like hydrogen bonding between the polymer segments and substrate surface, it is unclear if sufficient driving force for chain adsorption even exists in melts.

The kinetics of chain adsorption to a surface in solution has also been extensively studied.^{34,37,38} The complete adsorption process involves a number of steps: starting with bulk mass transfer of chains diffusing to the surface; the “sticking” of chains to the surface, a largely unknown process, but assumed to be very fast; subsequent changes in chain conformation of surface attached chains; and finally the exchange of surface chains with those in solution. Migration and detachment of surface attached chains are considered the slowest processes such that significant non-equilibrium effects are often observed experimentally. Initial chain adsorption to a bare surface is often treated as a “parking problem” where the first chains impinging on the surface are thought to spread out and maximize the number of segment–surface contacts made, while subsequent chains are left to occupy smaller “footprints” on the surface, filling in the remaining adsorption sites.^{39,40,57,58} This has led to the view that there can be two populations of surface attached chains, one “tightly” bound with many surface contact points per chain and the other more “loosely” bound.^{38,57} Some experimental evidence supports this view where exchange experiments have observed two stages to desorption, an initial rapid decrease in the population of surface attached chains followed by a slower decrease at longer times, interpreted as an initial desorption of more “loosely” bound chains followed by a slower desorption of the more “tightly” bound population.^{38,55,59} However, extensive studies by Granick et al. have found that this desorption rate can depend substantially on how long after the newly adsorbed layer was formed that the exchange experiment was started.^{55,60} It appears that an extensive surface residence time of many hours can be required to equilibrate adsorbed layers in solution,⁶⁰ substantially longer than the rapid time to reach constant adsorbed amount Γ ,³⁸ during which the number of contact points per chain will evolve. These experimental challenges of determining whether the system is in equilibrium or not substantially complicate comparisons with theory that typically assume equilibrium conditions.³⁸

A related conundrum has been the question of whether adsorption is reversible or irreversible, which was already deemed a long-standing dispute more than 30 years ago.³⁵ The classic argument for irreversibility is based on a Boltzmann factor and has the following reasoning:³⁵ For a given adsorbed chain with N segments, some fraction f of these segments will be in contact with the surface. Even if this fraction is small ($f \sim 0.1$), the probability of all fN segments detaching from the surface at once is

exponentially small, $\sim e^{-fNU_b/kT}$, where U_b represent the appropriate sticking energy per segment. As de Gennes stated in his 1987 review,³⁵ “this argument is utterly wrong”, as it assumes that chain desorption must occur with all segments detaching simultaneously. However, there is nothing preventing chains from desorbing piecemeal, by unzipping from the surface with the fN bound chain segments being slowly replaced by segments from different chains.^{60,61} By no means would the displacement of all fN bound segments occur quickly, and certainly some segments will detach and reattach multiple times, but as individual segments exchange readily over time, an adsorbed chain could easily detach from the surface and drift away into the solution. Studies by Douglas and Granick have shown that the rate limiting step is frequently diffusion of the chain away from the surface and not the energetics of surface detachment.^{62,63}

This view of reversible adsorption is supported by numerous experiments.^{34,37,59,61,64} Some of the most compelling are exchange experiments with isotopically labeled chains of equivalent molecular weight, where the concentration of radioactive chains on the surface decreases with time as equivalent, but non-radioactive chains in solution exchange with those on the surface.^{59,64} The original experimental support for the concept of irreversible adsorption was based on observations that the total adsorbed amount Γ at the surface is strongly conserved and does not decrease when adsorbed layers are rinsed with pure solvent. However, as explained by de Gennes,³⁵ this constancy of Γ does not represent irreversibility of adsorbed chains, but instead a strong driving force to maintain the saturation of chains at the surface in equilibrium. Even though the total adsorbed amount Γ is strongly conserved, individual chains can readily exchange.^{38,61} Experiments by van der Beek et al.^{65,66} have demonstrated that the displacement of surface bound chains can even be driven by small molecules if the “displacer” has a stronger binding energy u_s^0 to the surface than the bound polymer segment u_s , thereby reducing the adsorption energy parameter χ_s representing the difference in binding energy between the polymer segment and solvent molecule.³⁶

Granick’s group has done some of the most extensive characterization of the surface mobility of adsorbed chains. Direct measurements of the surface diffusion of adsorbed chains have demonstrated that surface bound chains in solution are extremely mobile.^{54,61,67–69} As would be expected, surface rearrangements occur more readily for weakly bound chains, compared to more strongly adsorbed chains.⁴⁰ The surface mobility of chains also depends on surface coverage where molecular crowding of chains on the surface can strongly reduce the measured diffusion constant.⁶⁷ Surface hopping of chains that detach and reattach to the surface some distance away has been directly observed with weakly bound chains.^{68,70} Even for strongly adsorbed chains with sticking energies greater than kT , chain diffusion across the surface can be readily measured.^{54,69} These strongly adsorbed systems demonstrate crawling of surface bound chains with a heterogeneous distribution of diffusion coefficients reflecting a range of chain mobilities associated with varying fractions of bound segments per chain. A given bound chain “may be adsorbed firmly even though the individual repeat units are in thermal equilib-

rium between the adsorbed and unadsorbed states”, meaning even strongly bound chains change conformation readily.⁶¹ The picture that emerges from all these experiments is that individual repeat units are not irreversibly attached, but instead, taken as a whole, the adsorbed layer in equilibrium is in essence “irreversibly” present on the surface because of the strong driving force to maintain a constant surface coverage Γ .³⁵

As is evident, there is a disconnect in conceptual understanding and interpretation between this older literature on chain adsorption in solution and the more recent literature on forming adsorbed layers by solvent washing melt films. We find that there is much experimental evidence from this older literature of how mobile adsorbed chains are in solution that invalidates the Guiselin assumptions in his proposed thought experiment. In particular, chains are not irreversibly adsorbed at the polymer segment level, but change conformation readily in solution even for strongly bound chains.

2 Experimental Methods

Silicon wafers were cleaned with one of three different procedures, all commonly used in the literature. Following most studies on chain adsorption,^{4,19,20,22,27} piranha cleaning was done by submerging silicon wafers in a mixture of 70% by volume H_2SO_4 and 30% by volume H_2O_2 (which is itself 30 vol% H_2O_2) for 30 min, with the temperature of the solution kept between 100–120 °C. Piranha solution is a strong oxidizer commonly used to remove organics and hydroxylate the surface. After removal from the solution, the substrates were rinsed liberally in hot deionized (DI) water, then dried with N_2 gas and placed in a closed clean container. Efforts were made to spin-coat polymer films onto these substrates within 10 min to minimize substrate recontamination. Alternatively, silicon wafers were cleaned with 10 vol% hydrochloric acid (HCl) for 30 min,⁵¹ before being rinsed liberally and sonicated in DI water for 5 min, then dried with N_2 gas and spin-coated within ~ 1 min. This acid cleaning procedure also removes organics and hydroxylates the surface, but is safer and logistically easier than piranha cleaning. As we demonstrate, both these acid cleaning procedures give comparable results of $h_{\text{ads}}(t)$. Some samples were also simply cleaned using toluene by dropping the solvent onto the spinning silicon wafer immediately prior to spin-coating to remove organic contaminants and dust from the surface. This limited toluene cleaning procedure is common to much of the literature on T_g confinement and other property changes in thin films when no cleaning procedure of silicon wafers is specified. It effectively recognizes that silicon wafers from the manufacturer come extremely clean, in most cases packaged in a cleanroom environment.

Polystyrene ($M_w = 400$ kg/mol, $M_w/M_n = 1.06$, Pressure Chemical) was dissolved in toluene and spin-coated onto the cleaned (2 cm \times 2 cm) Si wafers to create 200+ nm thick films. To be consistent, all samples were spin-coated at 800 rpm from 2.5 wt% solutions. However, we do not believe that differences in spin-speed or solution concentration would have a big impact on the measured adsorbed layer thickness h_{ads} formed after solvent washing because the compilation of $h_{\text{ads}}(t)$ results shown in Figure 1 are rather consistent (especially Fig. 1b) and come from a number of

different groups who would not have all used the same spin-speed and concentration. We do note that a recent study by Napolitano et al.¹⁸ has shown that $h_{\text{ads}}(t)$ values do decrease with decreasing film thickness for very thin films, $h < 5\text{-}10R_g$, which is why we have consistently started with bulk 200+ nm thick films, which are $> 10R_g$ for our 400 kg/mol M_w . Samples were then annealed for 0–50+ h at 150 °C or 120 °C under vacuum, or stored at room temperature. To remove the PS film and create adsorbed layers, annealed samples were then subjected to an iterative washing procedure,^{4,19,20,26,27} with one to three toluene washings, each performed by submersing samples individually in 50 or 100 mL of toluene for 30 min in covered glass containers. After washing, samples were blown dry with N_2 gas prior to being measured by ellipsometry.

Spectroscopic ellipsometry (Woollam M-2000) was used to determine the film thickness h_{ads} of adsorbed layers. Measurements were done at three angles of incidence from 55° to 65° every 5°, after being aligned at 65°, where data at different angles were fit simultaneously. The $\Psi(\lambda)$ and $\Delta(\lambda)$ data for $\lambda = 400 - 1000$ nm were modeled using a standard three layer optical model comprised of a Cauchy layer, $n(\lambda) = A + B/\lambda^2 + C/\lambda^4$, for the polymer film atop a Si substrate with a 1.32 nm native oxide layer, where this native oxide thickness was determined from the average of measurements on three 4-inch diameter wafers at five different points. Because ellipsometry has difficulty independently resolving thickness and index of refraction for very thin films less than ~ 10 nm,^{29,71} the index of refraction was held constant at values of $A = 1.563$, $B = 0.0079$, and $C = 0.00038$, based on an average over multiple PS films of bulk thickness.²⁸ Note, these Cauchy parameter values of A , B , and C are quoted for the wavelength λ in microns following the common convention used within the Woollam software.

3 Results and Discussion

We now evaluate experimentally the reproducibility and reliability of forming adsorbed layers by solvent washing melt films, following the most commonly used protocol in the literature (depicted in Fig. 2). Section 3.1 starts with ascertaining the reliability of using ellipsometry to accurately measure the absolute thickness of h_{ads} corresponding to very thin films $\lesssim 10$ nm, as well as the accuracy with which zero thickness of h_{ads} can be verifiably established. From these control tests we determined that a single measurement of h_{ads} is accurate to within ± 0.2 nm (which defines the symbol size used for h_{ads} in all subsequent figures), and that an adsorbed layer thickness h_{ads} below 0.24 nm is impossible to distinguish from zero. This minimum adsorbed amount we find reliably measurable is represented by a gray bar at a level of $h_{\text{ads}} = 0.24$ nm in Figures 4, 5, 7 and 8. Section 3.2 then addresses the reproducibility and reliability of creating $h_{\text{ads}}(t)$ curves as depicted in Fig. 1a following the experimental protocols outlined in the literature. We discuss the various experimental factors found to affect this process and provide some interpretation for the unexpected variability. Section 3.3 continues with addressing the impact of multiple solvent washing stages, as well as the initial substrate preparation and cleaning method. Section 3.4 evaluates the film average glass transition temperature $T_g(h)$ and physical

aging rate β for $h \approx 30$ nm thick films made with and without varying h_{ads} layers. We end with a summary and discussion of the implications of our findings with respect to the existing literature in thin films and polymer nanocomposites, and provide an outline of open questions still remaining to be addressed.

3.1 Reliability of Measuring Adsorbed Layer Thickness h_{ads} with Ellipsometry

As we are interested in investigating the reproducibility of forming adsorbed layers, we start by determining the accuracy and error with which ellipsometry can reliably measure the absolute thickness h_{ads} of such thin films. It is well known that ellipsometry has difficulty accurately measuring very thin films $\lesssim 10$ nm because the signal becomes primarily determined by the reflection at the interfaces when the path length of the light through the film becomes much less than the wavelength λ , minimizing the dispersion (wavelength dependence) contribution to the change in polarization.^{29,71} This is often illustrated using Δ vs. Ψ plots where, for a given angle of incidence, the trajectories of different curves, corresponding to different refractive index values of the film, converge to the same film-free point as the film thickness decreases to zero.⁷¹ We address this limitation by measuring three different angles of incidence (55° , 60° , 65°) for each sample, and globally fitting $\Psi(\lambda)$ and $\Delta(\lambda)$ values at all three angles for the wavelength range $\lambda = 400 - 1000$ nm to an optical layer model of a PS film on silicon. Following what is typically done for very thin films ($h \lesssim 10$ nm), we hold the index of refraction $n(\lambda)$ Cauchy parameters fixed at the bulk value.

Since there is always some uncertainty with which bulk refractive index values can be known, one could ask how sensitive the measured h_{ads} values are to the particular bulk value used. The Cauchy parameter values we determined from an average of multiple bulk samples have average and standard deviations of $A \pm \Delta A = 1.563 \pm 0.004$ and $B \pm \Delta B = 0.0079 \pm 0.0004$. (As the fitting is quite insensitive to the Cauchy C parameter, it was simply held fixed at the bulk value, $C = 0.00038$, although it quite reasonably could have been held fixed at zero too.) When we vary the Cauchy A and B parameters within one standard deviation of their bulk values ($\pm \Delta A$, $\pm \Delta B$), we find the measured values of h_{ads} vary by less than ± 0.01 nm. This demonstrates that the best fit values for h_{ads} are not particularly sensitive to the specific refractive index values chosen, assuming they are appropriate bulk values. We note that some works have suggested that adsorbed layers could have different properties from bulk, e.g., increased density,^{3,4,7,20,26,72} such that the choice of using bulk values for $n(\lambda)$ parameters may not be the most appropriate. However, given that these suggested property differences are still uncertain, bulk refractive index parameters seem to be the most reasonable to use. The choice of bulk parameters is supported by the works of Napolitano et al.^{14,18} and Tsui et al.²⁷, which demonstrated film thickness values for adsorbed layers measured by AFM gave the same results to those measured by ellipsometry using a fixed *bulk* value for $n(\lambda)$ during their layer model fitting. We have also done some AFM measurements verifying that h_{ads} thickness values by ellipsometry match. However, with its larger

spot size, ellipsometry does a better job of characterizing the adsorbed layer thickness across the sample surface than AFM which is restricted to a small area. We do note that similar to previous reports we observe some dewetting of the h_{ads} layers after solvent washing.^{20,22,73} All together these holes make up less than 10 % of the total surface area for very thin films < 4 nm, and less than 1 % of the total surface area for thicker films. The ellipsometer beam size on the sample spans a few mm by few mm thus easily averaging over these small holes.

It is well known that the largest instrument error associated with measuring the absolute film thickness with ellipsometry is often associated with the precision with which the angle of incidence to the sample is known.^{29,74} As this angle can be readily affected by sample tilt and alignment that can easily vary slightly from measurement-to-measurement or sample-to-sample due to anything from dust on the back of the sample to an individual researcher's alignment protocol, a series of different samples were measured repeatedly under varying conditions. We found that the error associated with measuring the thickness of a single sample is ± 0.13 nm on average with a maximum value of ± 0.17 nm. Thus, we conservatively conclude that the error in h_{ads} for any given measurement of a sample is ± 0.2 nm, and have consequently chosen to depict the size of the symbols (error bars) associated with any single measurement of h_{ads} as this value on the figures in this study.

Another point of consideration is the uncertainty associated with measuring zero h_{ads} adsorbed layer thickness, particularly because we aim to characterize the presence or absence of adsorbed layers. All silicon wafers have a native oxide layer that naturally forms when the silicon is exposed to oxygen in the atmosphere. Although technically this native oxide layer has a gradient composition, it is typically fit in ellipsometer optical layer models as a homogeneous SiO_x layer atop the silicon with a thickness varying between 1-2 nm in the literature. We specifically measured the thickness of the native oxide layer of our silicon wafers to be $h_{\text{SiO}_x} = 1.32 \pm 0.03$ nm (based on an average of five measurements each at different locations on three different 4-inch diameter wafers) using a homogeneous SiO_x layer with standard optical constants from Ref. 75 provided by Woollam in our ellipsometer software. This h_{SiO_x} value was for a single batch of silicon wafers at one point in time. Our lab has also previously done this test a few years prior finding²⁸ $h_{\text{SiO}_x} = 1.25$ nm and several years before that measuring⁷⁶ $h_{\text{SiO}_x} = 2$ nm. Thus, for any given batch of silicon wafers (all purchased from the same supplier), it would not be unusual for the SiO_x native oxide layer thickness h_{SiO_x} to vary between 1.25-2 nm. As the refractive index parameters for SiO_x are not that distinct from that for the polymer, a variation in the native oxide layer thickness h_{SiO_x} will affect the measured adsorbed layer thickness h_{ads} , especially influencing the thickness of h_{ads} that would be considered zero. If we take a bare silicon wafer, for which we know there is no adsorbed polymer, and vary the h_{SiO_x} layer thickness in the optical model between 1.25-2 nm, we find that the optical model fit returns an adsorbed layer thickness h_{ads} of up to 0.24 nm. Thus, we conclude that any adsorbed layer thickness h_{ads} below 0.24 nm is impossible to distinguish from natural variations in the native oxide layer thickness. We

note that this value is close to, but above the ± 0.2 nm error we determined above for a single ellipsometry measurement of h_{ads} . To indicate this uncertainty in measuring zero h_{ads} adsorbed layer thickness, we have added a gray bar to Figures 4, 5, 7 and 8 at a level of $h_{\text{ads}} = 0.24$ nm, which represents the minimum adsorbed amount we find reliably measurable.

3.2 Reproducibility of Measuring Adsorbed Layer Thickness

h_{ads}

With a solid foundation from Section 3.1 of how reliable a single ellipsometry measurement of h_{ads} is and how accurate zero thickness can be determined, we proceed now with evaluating the reproducibility of forming adsorbed layers by solvent washing melt films. We follow the sample preparation protocol depicted in Figure 2 representing that most commonly used in the literature with h_{ads} evaluated as a function of annealing time at an elevated temperature above T_g . Figure 4 shows a plot of adsorbed layer thickness h_{ads} versus annealing time at 150 °C under vacuum for PS films (>200 nm thick, $M_w = 400$ kg/mol, $M_w/M_n = 1.06$) spin-coated onto piranha cleaned silicon wafers. Each open symbol in the graph represents an individual sample where the value h_{ads} measured by ellipsometry was determined after a single wash of the sample for 30 min in 100 mL of toluene (a good solvent). This corresponds to the solvent washing procedure most frequently used in the literature that uses either one 30-min wash or 3+10-min washes in toluene.^{4,14,16,22,26,27} We have verified that a single 30 min wash gives the same final adsorbed layer thickness h_{ads} as three repeated washings of 10 min each.

Because of experimental limitations in the number of 2 cm × 2 cm silicon wafer pieces that can be piranha cleaned at one time, samples were prepared in batches with a maximum of 15 samples at a time. The maximum batch size was dictated by safety concerns about the amount of acid being used, as well as the logistics of minimizing the time between cleaning and spin-coating in order to prevent possible contamination of the freshly cleaned substrates. Batch sizes were also frequently smaller than the maximum batch size to help better control the quality of samples. In Figure 4, three batches have been highlighted in orange, cyan, and magenta, where data from additional batches are simply shown in gray. Dashed curves have been drawn to guide the eye through the trends of each highlighted batch. Although all batches show a similar trend, there is considerable variability from batch to batch, even though all were collected under nominally identical conditions. This batch-to-batch variability is noticeably larger than the ± 0.6 nm error in sample-to-sample reproducibility within a batch (see discussion below of Fig. 8) and the ± 0.2 nm single measurement error described above. Although the different batches in Figure 4 show qualitatively similar trends, there is significant quantitative differences such that a quantified $h_{\text{ads}}(t)$ trend determined from an analysis of the data would be highly dependent on the amount of data and, in particular, the number of batches collected.

To overcome this batch-to-batch variability in order to quantify trends in $h_{\text{ads}}(t)$, we bin together the data for similar annealing times from different batches, where the solid blue data in Fig-

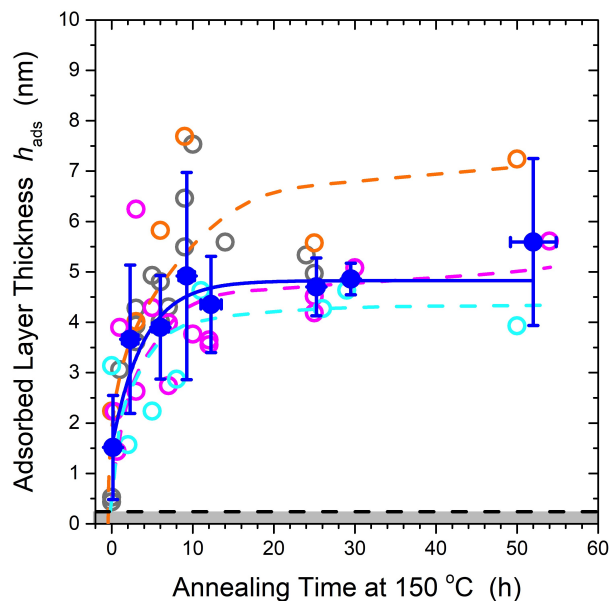


Fig. 4 Reproducibility of the measured adsorbed layer thickness h_{ads} as a function of time the film was annealed at 150 °C under vacuum prior to solvent washing for 30 min in toluene. Data are for PS films (>200 nm thick, $M_w = 400$ kg/mol) spin-coated onto piranha cleaned silicon wafers, where the symbol size represents the error of ± 0.2 nm for an individual ellipsometry measurement of h_{ads} , while the gray bar and dashed line across the bottom of the graph represent the uncertainty in measuring zero adsorbed layer thickness, $h_{\text{ads}} \leq 0.24$ nm. Open symbols highlighted in orange, cyan, and magenta are for individual batches of samples that were piranha cleaned and measured together, where dashed curves are drawn to guide the eye through the trends in the individual batches. Gray open symbols represent data from other batches collected. Solid blue symbols and associated error bars are the average and standard deviation for all batches binned together where the solid blue curve is a fit to eq. 4, the most simple functional form used in the literature for $h_{\text{ads}}(t)$.

ure 4 represent the average and standard deviation of this binned data. The binned data show that the adsorbed layer thickness h_{ads} increases with increasing annealing time and saturates out at some long time value, consistent with literature reports as depicted in Figure 1.^{4,14,15,22,26,27} Following what seems most reasonable from other studies,^{1,4,15,22,26,27,30} we fit the solid blue binned data to a function of the form

$$h_{\text{ads}}(t) = \Delta h(1 - e^{-t/\tau}) + h_0 \quad (4)$$

to describe the increase in h_{ads} observed with increasing annealing time, where the long-term plateau $h_{\text{ads}}(t = \infty) = \Delta h + h_0$ is given by two constants. The initial thickness at zero annealing time, $h_{\text{ads}}(t = 0) = h_0$, accounts for the uncertainty in measuring zero adsorbed layer thickness as described above, and that not all polymer chains may be completely washed off even for films that were never annealed (as demonstrated below in Fig. 8). The best fit parameters for the blue curve shown in Figure 4 are $h_0 = 1.5 \pm 0.4$ nm, $\Delta h = 3.3 \pm 0.4$ nm, and $\tau = 4 \pm 1$ h, with the long-term plateau corresponding to $h_{\text{ads}}(t = \infty) = \Delta h + h_0 = 4.8 \pm 0.8$ nm. Note that if the individual batches are fit separately to eq. 4, the variability in the parameters would be significant, with τ varying

by more than an order of magnitude.

When we first started to reproduce curves of $h_{\text{ads}}(t)$ following the basic literature protocol outlined in Figure 2, we did not get as reproducible data as shown in Figure 4. Figure 5 shows a second graph of adsorbed layer thickness h_{ads} versus annealing time at 150 °C where the black open symbols are data collected by two separate people following the Fig. 2 literature protocol, but without particular attention paid to collecting data in consistent batches with progressively increasing annealing time within the batch. The data shown in Figure 5 were often collected under conditions where several samples within a batch were intended to fill-in data on the graph at particular annealing times. For efficiency, it was common to solvent wash a group of samples at the same time resulting in samples frequently being left in a drawer overnight (or even a weekend) after or even prior to annealing at 150 °C for a few hours. As can be seen in Figure 5, this produces $h_{\text{ads}}(t)$ values with considerably more scatter than that shown in Figure 4. (For reference, the blue binned data of Fig. 4 are also plotted on Fig. 5.) After considerable sleuthing, we determined that time spent by samples ‘sitting in a drawer’ either prior to or after annealing at 150 °C, before solvent washing, have a large and reproducible impact on the measured h_{ads} thickness after solvent washing. Figure 5 highlights purple data for which the time spent by the samples ‘sitting in a drawer’ prior to annealing at 150 °C was systematically increased from zero to 3, 6, 9, 24 hours (open-crossed diamonds) and 48 hours (solid diamonds), where the data clearly show a progressive increase in h_{ads} thickness with increasing time ‘sitting in a drawer’. For these samples, we specifically ensured that the samples were solvent washed immediately after annealing at 150 °C. We separately found that time ‘sitting in a drawer’ after annealing at 150 °C also tended to increase the measured h_{ads} thickness after solvent washing. In contrast, the data shown in Figure 4 are for samples where we specifically ensured that the samples were not left ‘sitting in a drawer’ either prior to or after annealing at 150 °C.

What is particularly perplexing about the purple data highlighted in Figure 5 where the samples were simply left in a drawer prior to annealing at 150 °C, is that one would expect that the extended annealing at 150 °C, a temperature well above T_g , would erase all thermal history of the sample. It is well known that glassy polymer films undergo physical aging (densification) as a function of time, even at room temperature ‘sitting in a drawer’. Typically in experimental studies we do not pay particular attention to this because the amount of aging that occurs is minimal and most experiments start with an annealing step immediately prior to data collection to reset the thermal history of the sample. However, in this case, we find that this aging at room temperature has an impact on the ability of the solvent to wash away the film. We can rationalize this observation by recognizing that the ability of the solvent washing step to remove chains from the glassy polymer film will depend on how much the film has densified.

Dissolving of glassy polymer films with solvent typically occurs through a Case-II diffusion process^{41,77–79} where the solvent must first penetrate and swell the glassy material through a diffusion front before there is sufficient mobility of the chains to be dissolved away. The speed of this dissolution process will be re-

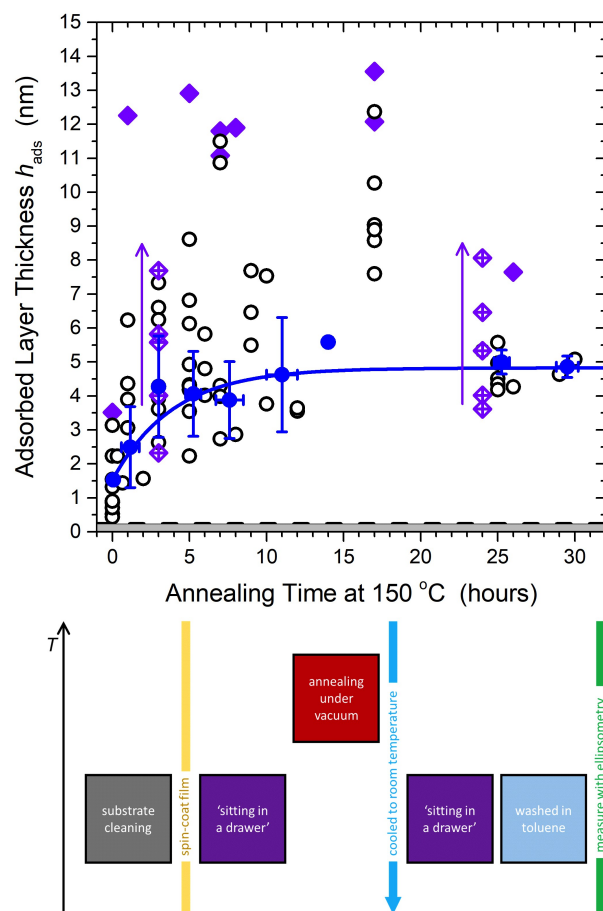


Fig. 5 Wider range of adsorbed layer thickness h_{ads} data (black open circles) plotted as a function of time the film was annealed at 150 °C under vacuum prior to solvent washing for 30 min in toluene, where no particular effort was done to make the samples in batches or minimized the time between steps in the experimental protocol outlined in Fig. 2. In contrast, the solid blue data and error bars are the binned data from Fig. 4 where effort was made to minimize the time samples spent ‘sitting in a drawer’ either prior to or after the annealing step at 150 °C. Purple data highlight the increase in h_{ads} observed when the time spent ‘sitting in a drawer’ prior to the thermal annealing step is systematically increase from zero to 3, 6, 9, 24 hours (open crossed diamonds) and at 48 hours (solid purple diamonds). Again data are for PS films (>200 nm thick, $M_w = 400$ kg/mol) spin-coated onto piranha cleaned silicon wafers, where the symbol size represents the error of ± 0.2 nm for an individual ellipsometry measurement of h_{ads} , while the gray bar and dashed line across the bottom of the graph represent the uncertainty in measuring zero adsorbed layer thickness, $h_{\text{ads}} \leq 0.24$ nm.

duced for films that have undergone densification due to physical aging of the glassy film.^{80,81} For the purple data shown in Fig. 5, the time ‘sitting in a drawer’ prior to annealing at 150 °C occurs after spin-coating. These glassy films formed by a solvent quench initially contain a significantly reduced density as the glassy film solidified during spin-coating when solvent was still present in the film, after which the solvent evaporated leaving behind voids. Thus, these solvent-quenched glassy films would be expected to undergo a significant amount of densification over time ‘sitting in a drawer’. Similarly, films stored in a drawer after the annealing step at 150 °C will undergo physical aging after their thermal

quench to room temperature, also densifying over time.

Figure 6 compares the densification of bulk PS films after a solvent and thermal quench into the glassy state by plotting normalized film thickness h/h_0 as a function of aging time on a logarithmic axis. The solvent quenched data are for a sample placed on the ellipsometer at near room temperature (30 °C) immediately after spin-coating, while the thermally quenched data show a traditional physical aging curve at an aging temperature of 40 °C, a near room temperature value, and at 65 °C, where the maximum in aging rate occurs.^{74,82} Both curves in Figure 6 were normalized to their respective film thicknesses at 10 min after the quench process such that the y-axis provides a measure of the film's percentage decrease in thickness. Freshly spin-coated films show a large $\sim 3.5\%$ decrease in film thickness immediately after spin-coating, which is significantly larger than the $\sim 0.5\%$ decrease for film that undergo a thermal quench from the equilibrium liquid state. This is because spin-coated films undergo vitrification into the glassy state via a solvent quench while some solvent is still present in the film, which then evaporates out of the film leaving behind voids that then collapse over time. The thermally quenched film, in contrast, has no such voids and thus the resulting time-dependent densification after vitrification is much less. A similar comparison was published previously by Keddie et al.^{83,84} for solvent and thermally quenched PMMA films also demonstrating a much larger densification for solvent-quenched vs. temperature quenched films. Note that we chose to normalize the data in Fig. 6 at the $h(t)$ curve's initial value h_0 because this value is well defined. However, in the long time limit $h(t \rightarrow \infty)$ all curves tend towards the same equilibrium value for a given temperature,^{83,85} but as this long time equilibrium limit cannot be reached experimentally, it is less well defined.⁷⁴ The data in Fig. 6 should not be misinterpreted to imply that solvent quenched films are denser than thermally quenched films; in fact, the opposite is true.⁸³

We believe this densification of solvent-quenched films at room temperature explains why films with zero hours of annealing at 150 °C show a larger h_{ads} thickness if left 'sitting in a drawer' for some length of time. Such densification would significantly slow solvent penetration and swelling of the glassy film, making it harder to wash off. For a given 30-min solvent washing procedure, a larger h_{ads} layer would remain. This interpretation is consistent with data by Koga et al. (inset of Fig. 1 in Ref. 26) showing that the maximum adsorbed layer thickness reached at long times $h_{\text{ads}}(t = \infty)$ is independent of annealing temperature from 140 °C all the way down to 40 °C (near room temperature). These data demonstrate that annealing above T_g is clearly unnecessary to form adsorbed layers by solvent washing films off substrates.

The interpretation of why densification of solvent-quenched films when 'sitting in a drawer' prior to annealing at 150 °C also leads to larger h_{ads} thicknesses is less clear. By examining the data in Fig. 5, it appears that extended annealing of films at elevated temperatures above T_g (>20 h at 150 °C) leads to less variation in the residual $h_{\text{ads}}(t)$ thickness remaining after solvent washing, where perhaps the sample history of 'sitting in a drawer' prior to annealing is slowly erased. This slow evolution of the $h_{\text{ads}}(t)$ data at long annealing times is suggestive of a slow restructuring of

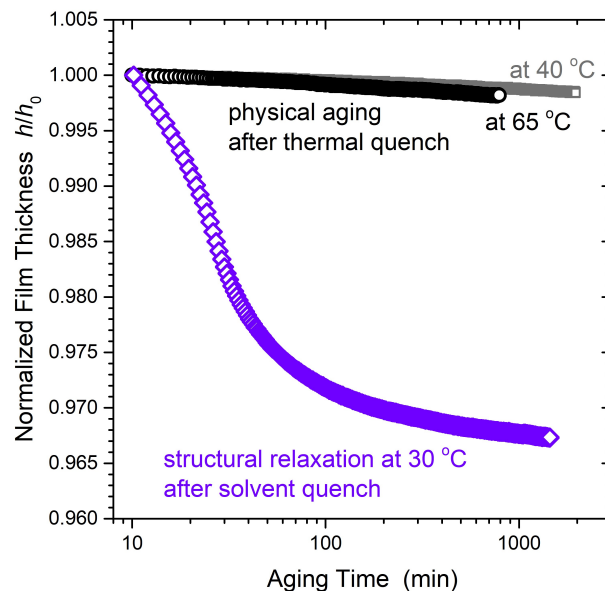


Fig. 6 Decrease in film thickness h , normalized to the initial thickness h_0 , observed for bulk PS films ($M_w = 400$ kg/mol) as a function of aging time demonstrating the densification of the film that occurs following a solvent quench (purple diamonds) where the film immediately after spin-coating was placed on the ellipsometer hot stage held at 30 °C, compared to an equivalent film that underwent a thermal quench from 120 °C to an aging temperature of either 40 °C (gray squares) or 65 °C (black circles), the temperature at which the physical aging rate is maximum.

chains within the film that may be occurring near the substrate interface, where perhaps the fraction of chains with monomers in contact with the substrate interface may be changing. It would be reasonable to conclude that films which were densified significantly after solvent quenching by 'sitting in a drawer' prior to being thermally annealed may have considerably slower exchange kinetics of monomers in contact with the substrate. Studies of chain diffusion near substrates have reported slower than bulk dynamics,^{86–88} which would be consistent with this interpretation. However, these $h_{\text{ads}}(t)$ values are for films that were rinsed with a specific solvent washing protocol (30 min in toluene), which makes the interpretation of any restructuring of chain conformations that could be occurring in the film during annealing indirect as what is actually being measured is the ability of this solvent washing protocol to swell and rinse off the glassy film resulting from this sample history and annealing protocol. A more direct approach to investigating such questions would be to directly measure the exchange kinetics at elevated temperatures with something like neutron scattering, an experiment which has been done recently by Kumar et al. for poly(2-vinyl pyridine) (P2VP) chains bound to silica nanoparticles.⁸⁹ For this strongly attractive hydrogen bonding system, they observed a strong temperature dependence where surface bound $d3$ -P2VP chains slowly exchanged with h -P2VP chains in the matrix over ~ 10 hours at 175 °C, but not after 1000 h at only 150 °C.

We recognize that our Figures 4 and 5 look substantially different from the $h_{\text{ads}}(t)$ curves previously shown in the literature, as summarized in Figure 1. This may be because other studies likely only collect one batch of data^{4,26,27,90} or only graph

binned data.^{14,15,22} The only statement we have found in the existing literature that acknowledges that some samples may not infrequently have much larger or different h_{ads} values is in a recent paper by Napolitano et al. that specifically discussed sample preparation and analysis details with a section on data handling stating:¹⁵

“In order to consistently obtain the adsorption kinetic parameters in Equation 1 [eq. 2 in Section 1.1], a number of steps is necessary for a proper analysis of the data sets (h_{ads} as a function of annealing time) experimentally determined. First, the quality of the data is significantly improved by averaging several measurements of samples prepared within identical conditions (annealing temperature, type of substrate) and history (same annealing times). When averaging, dataset clear outliers, e.g. resulting from improper handling of a sample, must be discarded. This can be achieved by fitting a single saturating exponential to the data (i.e. $h_{\text{ads}} = h_0 + \Delta h[1 - \exp(-t/t_{\text{ads}})]$ where $h_\infty = h_0 + \Delta h$ and t_{ads} is the characteristic time of the process) [eq. 4 above]. This fit can be used to eliminate outliers in the data set (i.e. $|h_{\text{ads}} - h_{\text{fit}}| > 3\sigma$), in addition to provide a good estimate of the equilibrium adsorbed thickness h_∞ . The uncertainty in the fit for h_∞ can be used to discard data-sets in which the annealing time was insufficient to achieve an equilibrium saturated value.”

This suggests to us that others have also observed considerable variability in the measured $h_{\text{ads}}(t)$ values after solvent washing, perhaps from similar variables we have described in this section, but have instead chosen to interpret it in a different manner. In our view, we would be concerned with this data analysis procedure described in the quoted text where $h_{\text{ads}}(t)$ data, perhaps comparable to those shown in Figures 4 or 5, were first fit to eq. 4 (a three parameter fit) and used to discard data which fall outside of 3σ , prior to performing a second fit on the remaining data to a more complicated two-stage functional form, eq. 2 with five fitting parameters.

From our experimental investigations, we find that the $h_{\text{ads}}(t)$ results are strongly impacted by the solvent washing protocol used and the prior history of the sample, consistent with the interpretation that denser films require longer for a given solvent to swell and wash off the glassy polymer film. Even though averaging and binning of data do result in much nicer looking $h_{\text{ads}}(t)$ curves closer to those compiled in Figure 1a, we question whether this protocol meaningfully reveals information about the state of the melt film prior to solvent washing. As we will demonstrate in the next section, continued solvent washing also further alters the measured $h_{\text{ads}}(t)$ values consistent with restructuring of the adsorbed polymer chains in solution as previously reported in the earlier literature.

3.3 Impact of Multiple of Washings and Substrate Cleaning Method on Adsorbed Layer Thickness h_{ads}

We look now at the impact of multiple solvent washings on the $h_{\text{ads}}(t)$ trends given that several studies,^{4,19,20,22,26,27} especially

those by Koga et al.,^{4,19,20,26} have done multiple washing believing these procedures to provide more information about the adsorbed layer structure. As it is logistically cumbersome to collect multiple batches of data each time, we proceed now with our discussion using only a single batch of data to represent the trends we observe recognizing that trends will be qualitatively similar if another batch were collected, but likely have quantitative differences. We also return now to the experimental protocol used in the collection of data for Figure 4 where we ensure samples were annealed and washed immediately after each step, without any time spent ‘sitting in a drawer’, the protocol which we believe produces data that most closely resembles that shown in the literature. Figure 7 shows the $h_{\text{ads}}(t)$ trend for a single batch of data upon repetitive washing, with the open, half-filled, and filled symbols representing the first, second, and third 30-min wash in 100 mL of fresh toluene, respectively. The curves shown, included as guides to the eye through each dataset, demonstrate that $h_{\text{ads}}(t)$ decreases progressively with each subsequent washing. This decrease in the adsorbed layer thickness with only a few increasing repetitions of washing indicates that the continued washing of annealed samples affects the final adsorbed layer amount, even those samples annealed for long times. However, the overall trend of increasing adsorbed layer thickness with increasing annealing time remains unchanged, indicating that at longer annealing times the removal of the polymer film by solvent washing is more challenging.

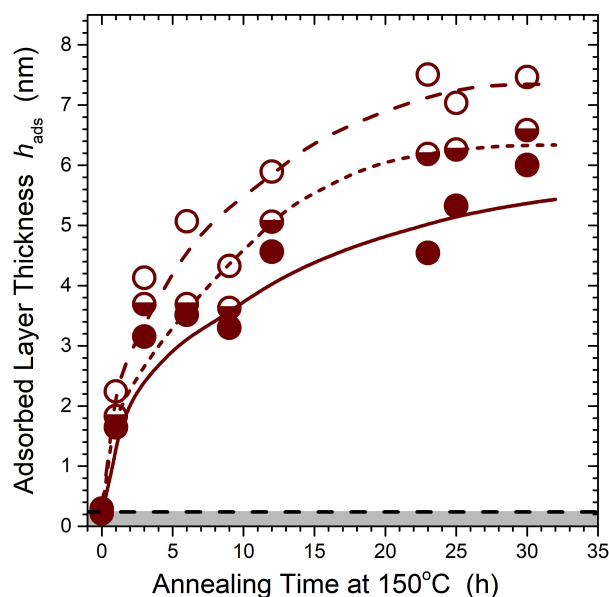


Fig. 7 Plots of the adsorbed layer thickness $h_{\text{ads}}(t)$ as a function of annealing time at 150 °C under vacuum for PS films (>200 nm thick, $M_w = 400$ kg/mol) on HCl acid cleaned silicon wafers (made as a single batch) where the films were subsequently solvent washed in 100 mL toluene for 30 min once (open circles), twice (half-filled circles), or three times (filled circles). The curves through the data are guides to the eye indicating the general trend of a progressive decrease in the $h_{\text{ads}}(t)$ curve with increasing number of washes. Again the symbol size represents the error of ± 0.2 nm for an individual ellipsometry measurement of h_{ads} , while the gray bar and dashed line across the bottom of the graph represent the uncertainty in measuring zero adsorbed layer thickness, $h_{\text{ads}} \leq 0.24$ nm.

These data naturally lead to the question that if only a few repetitive washings have such a significant impact on the measured $h_{\text{ads}}(t)$ adsorbed layer thickness, what does this procedure inform us about the state of the melt film prior to solvent washing? Proponents of chain adsorption in the melt argue that solvent washing films in a good solvent like toluene removes the unattached chains leaving behind only the “irreversibly adsorbed” chains.^{1,6,10,14–20} This is a procedure that has been termed “Guiselin’s experiment” or “Guiselin’s approach”, based on Guiselin’s theoretical assumption³² that chain segments in contact with the substrate interface in a film are irreversibly adsorbed and his proposition that solvent washing could remove unattached chains to access this adsorbed layer from the melt. Koga et al. argues that further solvent washing (150 days in toluene²⁶ or a couple of days in a stronger solvent such as chloroform⁴) “reveals” additional buried structure of the adsorbed layer in the melt that they have termed “flattened layers”.^{4,19,26}

The Guiselin paper cited³² is a theoretical study following the scaling analysis methods of Alexander⁹¹ and de Gennes⁹² for grafted chains in solution, where Guiselin uses similar scaling arguments to calculate the concentration profile of irreversibly adsorbed chains in a good solvent. To make the theoretical analysis possible, Guiselin assumes there are a set of chain segments permanently fixed to the surface, the set of which is determined by the random walk (Gaussian) statistics of chains in an initially concentrated solution or melt. The analysis relies on the theoretical assumption that all points in contact with the surface become permanently (or irreversibly) adsorbed, while all other chains not in direct contact with the surface can be removed without changing the initial permanent set of contact points. Guiselin proposes that this could potentially be achieved experimentally by washing out unattached chains with pure solvent, arguing this would be valid in the limit of strong adsorption sites.³² However, this theoretical case treated by Guiselin requires chains be sufficiently *mobile* in the initial concentrated solution or melt state to allow equilibrium Gaussian random walk chain conformations to be achieved, yet then be subsequently sufficiently *immobile* in the good solvent state to produce permanent, irreversibly adsorbed chain segments. Experimentally such a mobile-then-immobile situation could only be realistically achieved with some form of chemical bonding or grafting, as in the case of polydimethylsiloxane (PDMS) that can crosslink with silica substrates when heated to elevated temperatures, producing what is known as a “pseudo-brush”.⁹³

Durning and O’Shaughnessy³¹ appear to be the first to attempt an experimental realization of Guiselin’s mobile-then-immobile thought experiment, which they recognized would be “difficult to achieve in practice”. They stated:³¹ “In principle, one has to equilibrate the melt or dense solution against an inert solid surface and then, by some means, suddenly and permanently fix only the segments currently adsorbed.” For their experiments they selected a PMMA/quartz/benzene system because the segmental sticking energy would be of order several kT . PMMA films on quartz were annealed at 165 °C for up to 120 h in an argon atmosphere, and subsequently washed with benzene three times for 3 h, followed by sonicating for 5–10 min. The extended

annealing at 165 °C was believed to be necessary and sufficient to obtain reflected random walk statistics of chain conformations in the melt prior to solvent washing, with the hydrogen bonding between PMMA and the quartz surface then strong enough to prevent rearrangement of bound chains during solvent washing. A later review by O’Shaughnessy and Vavylonis⁹⁴ cautioned that these “experiments raise two important issues which deserve further study: (1) Guiselin’s thought experiment which envisions the instantaneous freezing-in of equilibrium melt configurations in practice may require annealing over large timescales for many experimental realizations. If the Guiselin predictions are to apply, this timescale, which depends on these unknown chain dynamics, must be large enough for any non-equilibrium configurations generated at the interface during melt deposition to have disappeared. (2) After swelling by solvent, one expects desorption–readsorption events and slow chain movements.”

Experimental works have shown that these two mobile-then-immobile requirements for Guiselin’s thought experiment are mutually exclusive, and appear to be experimentally unviable. The polymer solution literature summarized in Section 1.2 has extensively demonstrated that polymer chain segments adsorbed on a surface are extremely mobile, readily desorbing and readsorbing, even for the case of strong adsorption where the segment–substrate interaction strengths are several kT .⁵⁴ Experiments have measured the surface diffusion of adsorbed chains in solution translating across the surface via crawling and hopping mechanisms,^{54,67–70} and readily exchanging with other species in solution.^{34,36–38,40,59,61,64–66} Thus, it is well documented that the structure of surface bound chains and their segment–surface contacts change quickly in solution.

Rearrangement of segment–surface contacts in a melt state is more challenging to interrogate experimentally and many open questions remain. As argued in Section 1.2, the adsorption energy parameter χ_s as defined in most adsorption theories, eq. 3, would be strictly zero in a melt system with no solvent present; thus, simple analogies with solution treatments cannot be made. Certainly dynamics in a melt will be slower than that in solution. Several studies have demonstrated slower than bulk diffusion for PS chains near silica substrates,^{2,9,86–88} attributed to segment–surface contacts increasing the friction for reptation,^{86,87} with effects reaching extended distances from the interface.^{9,87} Most recently, Kumar et al. have investigated the exchange lifetime of surface bound P2VP chains to silica nanoparticles at elevated temperatures, with results suggesting that in such strongly favorable systems, surface bound chains can persist for weeks at 150 °C.⁸⁹ Dielectric measurements by Sokolov et al. have also found that the segmental mobility $\tau(T)$ of P2VP near silica nanoparticle interfaces is two orders of magnitude slower than bulk with a slightly weaker temperature dependence.⁹⁵ Thus, achieving equilibration of chain conformations in a melt state in the Guiselin sense seems doubtful.

The older literature on polymer adsorption in solution noted the importance of substrate cleanliness on the resulting adsorbed layer amounts, where Granick et al. in particular examined how various substrate treatments and cleaning methods altered the resulting chain adsorption.⁹⁶ This is also true for the h_{ads} thick-

nesses obtained from solvent washing melt films, as is shown in Fig. 1b, where HF treatment consistently results in larger h_{ads} layers than substrates cleaned with piranha solution, for a given nominally equivalent solvent washing procedure. HF treated silicon results in an altered surface chemistry of Si–H, while piranha cleaning simply oxidizes the organics on the surface such that they can be readily washed off with water, and thus leaves the SiO_x/Si surface chemistry of the silicon unchanged. The piranha solution is a mixture of concentrated H₂SO₄ and H₂O₂ that results in an exothermic reaction that can easily reach temperatures in excess of 120 °C, and as such it becomes highly hazardous and potentially explosive. Most publications actually note safety warnings associated with using piranha mixtures. We have found that HCl is a much safer acid mixture for substrate cleaning that also strongly oxidizes organics and leaves the silicon hydrolyzed. Figure 8 compares the adsorbed layer thicknesses h_{ads} measured after one, two, and three 30-min toluene washes for substrates cleaned with different methods. All films were vacuum annealed for 13 hours at either 150 °C or 120 °C, as indicated. The data demonstrate that our safer HCl cleaning method (30 min in 10 vol% HCl) is equivalent within error to the standard piranha cleaning procedure commonly used in the adsorption literature for samples annealed at both 150 °C and 120 °C, resulting in the same h_{ads} thickness after solvent washing. Data shown are the average of four samples with the error bars drawn in the figure representing the average sample-to-sample variability within a batch. We find this sample-to-sample error decreases progressively from ± 0.6 nm to ± 0.4 nm and ± 0.2 nm for one, two, and three toluene washes, respectively. We recognize that for the 150 °C annealed samples, the HCl cleaned substrates appear to result in slightly reduced h_{ads} thicknesses on average, albeit with overlapping sample-to-sample error bars. The more proper error for this comparison would probably be the batch-to-batch error of ± 1 nm, which would make the data for these two substrate cleaning procedures more equivalent. Given that the adsorbed layer thicknesses are the same and because HCl is safer and easier to use than piranha cleaning, Figure 7 was collected with HCl cleaned substrates.

Relevant to our discussion below that considers the impact of these $h_{\text{ads}}(t)$ studies on nanoconfinement investigations in thin films, in Figure 8 we also examined substrates that were toluene cleaned. Much of the literature on nanoconfined systems cleans silicon substrates by simply rinsing the silicon with toluene immediately prior to spin-coating the film. This minimalistic cleaning procedure is justified because silicon wafers come from the manufacturer pre-cleaned typically with some type of acid oxidizing solution and then packaged in a clean room environment. The most common annealing procedure followed in nanoconfinement studies is overnight under vacuum at $T_g^{\text{bulk}} + 20$ °C, which for PS with $T_g^{\text{bulk}} = 100$ °C means 120 °C. In our lab, over the years “overnight” has meant anywhere from 13–18 h. This explains our choice in Figure 8 for comparing annealing conditions at 120 °C for 13 hours, while the temperature of 150 °C is that most commonly used in the adsorption literature for PS. Compared to the more aggressive piranha and HCl cleaning procedures, toluene cleaned substrates lead to consistently smaller residual adsorbed

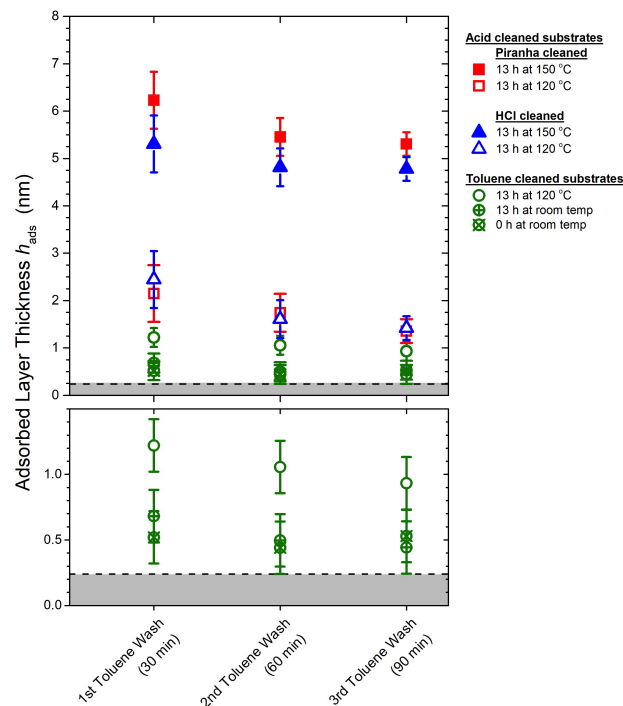


Fig. 8 Comparison of the adsorbed layer thickness h_{ads} after one, two, or three 30 min washes in 100 mL of toluene, following 13 hours of annealing under vacuum at either 150 °C, 120 °C, or simply sitting at room temperature, on silicon substrates cleaned with either piranha solution (red squares), HCl acid (blue triangles), or simply toluene (green circles). Data shown represent the average and standard deviation of four samples each, and the gray bar with dashed line across the bottom of the graph represent the uncertainty in measuring zero adsorbed layer thickness, $h_{\text{ads}} \leq 0.24$ nm. The bottom portion is a zoomed in version of the toluene cleaned data.

layer thicknesses h_{ads} under the same annealing and solvent washing conditions. The average sample-to-sample variability within a batch for the toluene cleaned data are noticeably smaller than what was observed for the piranha and HCl cleaned substrates, in most cases these were around ± 0.16 nm. As this would be smaller than the ± 0.2 nm error that we previously identified as the error for the ellipsometry measurement itself, we therefore opted to graph ± 0.2 nm for the error bars of the toluene cleaned data. It is clear that chain adsorption appears to be much less prevalent on toluene-cleaned compared to acid-cleaned substrates, which implies that in much of the nanoconfinement literature polymer adsorption is likely significantly less prevalent than suggested by chain adsorption studies done on acid-cleaned substrates and annealed under more aggressive conditions. We believe this strong impact of substrate cleaning method likely explains the slower growth and different shape of $h_{\text{ads}}(t)$ observed by Napolitano et al. in Figure 1a, which are for samples that were cleaned using organic solvents.¹⁵

Given the discussion associated with Figure 5 about the unexpected observations that time ‘sitting in a drawer’ had impact on the measured adsorbed layer thickness h_{ads} after solvent washing, we also include in Figure 8 data for films that were spin-coated onto toluene cleaned substrates and then left ‘sitting in a drawer’ overnight for 13 hours. Again this would not be an unusual cir-

cumstance given that experimentally it is common practice to leave samples ‘sitting in a drawer’ between measurements. As the h_{ads} thicknesses for toluene cleaned substrates are exceptionally small, we magnify this data in the lower region of Figure 8. We find that these samples never annealed above T_g , but left ‘sitting in a drawer’ at room temperature for 13 h, have roughly the same small adsorbed layer thickness $h_{\text{ads}} \approx 0.5$ nm, as samples simply spin-coated and washed off toluene cleaned substrates immediately. Tsui et al. previously measured the residual thickness h_{ads} for PS films spin-coated onto either piranha cleaned or HF treated silicon and immediately washed off, as a way to verify their solvent rinsing procedure, claiming $h_{\text{ads}} = 0$ was achieved for films that were never annealed.²⁷ We find the residual thickness h_{ads} after such a procedure is very small $h_{\text{ads}} < 0.5$ nm, but non-zero. This naturally leads to the question of what h_{ads} thickness should be properly considered $h_{\text{ads}} > 0$. As described above in Section 3.1 on the reliability of measuring h_{ads} with ellipsometry, we determined that values of $h_{\text{ads}} \leq 0.24$ nm should be reasonably considered as $h_{\text{ads}} \approx 0$ because it would be impossible to distinguish from natural variations in the native oxide layer thickness. In Figure 8, we depict this uncertainty in measuring zero h_{ads} adsorbed layer thickness as a gray bar. While the toluene cleaned data for samples that were never annealed above T_g come close to this h_{ads} minimum of 0.24 nm, they are still notably above it outside of experimental error. This observation is consistent with the literature on polymer adsorption in solution, where if you were to dip a clean silicon wafer into a dilute polymer solution, chains would naturally adsorb to the substrate leaving behind a small, but non-zero h_{ads} thickness.³⁴ This older literature established that even though polymer chains adsorbed on the substrate interface are quite mobile and can readily exchange with those in solution, there is an equilibrium adsorbed amount quickly reached in solution with a strong restoring force to maintain this surface saturation condition by balancing adsorption/desorption rates.³⁵

3.4 Impact of Adsorbed Layers on Film Average $T_g(h)$ and Physical Aging

Much of the recent literature on adsorbed layer formation in melt films has correlated measurements of the residual layer thickness $h_{\text{ads}}(t)$ after some given annealing and solvent washing conditions, with parallel measurements on samples showing changes in film properties and dynamics under equivalent annealing treatments.^{1–13} From this comparison, studies have argued that chain adsorption formed in the melt during this annealing process is responsible for numerous changes in nanoconfinement effects such as altering $T_g(h)$ reductions,^{1,6,8,21,22} increasing viscosity,^{2,9} and altering other properties in thin films.^{5,10,16,20,24} Such a comparison on nominally equivalent, but different samples assumes that $h_{\text{ads}}(t)$ is a reliable and meaningful measure of some characteristic of the melt film prior to solvent washing. However, based on our observations, the adsorbed layer thickness h_{ads} seems to be largely determined by the solvent washing conditions used to expose it. Thus, to try and ascertain the impact of h_{ads} layers on melt film properties, we directly test the impact of different adsorbed layer thicknesses on the average glass transition temperature $T_g(h)$ and

physical aging rate $\beta(h)$ of thin films by first explicitly forming a given adsorbed layer thickness h_{ads} following the protocols we elucidated above, and then embedding this known h_{ads} layer into a melt film.

In Figure 9, we compare the average $T_g(h)$ and $\beta(h)$ of $h \approx 31$ nm thick films that were formed by floating a PS layer of thickness h_{float} atop a previously formed adsorbed layer of a given thickness h_{ads} to create a total film thickness of $h_{\text{total}} = h_{\text{ads}} + h_{\text{float}} \approx 31$ nm. Specifically, in Figure 9 we compare (i) $h_{\text{total}} = 34.2$ nm with $h_{\text{ads}} = 6.9$ nm, (ii) $h_{\text{total}} = 33.1$ nm with $h_{\text{ads}} = 3.2$ nm, and (iii) a “regular” film of $h_{\text{total}} = 30.3$ nm ($h_{\text{ads}} = 0$) directly spin-coated onto a toluene-cleaned bare silicon substrate. The explicit preformed adsorbed layers were made by annealing bulk (>200 nm) PS films on HCl cleaned silicon under vacuum at 150 °C for either 23 h ($h_{\text{ads}} = 6.9$ nm) or 3 h ($h_{\text{ads}} = 3.2$ nm) and then rinsing once in toluene for 30 min, equivalent to the most common procedure used to make adsorbed layers from melt films. After capping with the additional PS layer, the $h_{\text{total}} = h_{\text{ads}} + h_{\text{float}}$ films were annealed for 2 hours at 170 °C under vacuum in an attempt to ensure good chain interpenetration between the top PS layer and underlying adsorbed layer. These annealing conditions used for merging the $h_{\text{ads}} + h_{\text{float}}$ layers were chosen to match our recent work where we capped end-tethered PS chains to investigate local T_g changes near the grafted substrate interface,⁵¹ the conditions of which were based on literature studies for the interpenetration of end-grafted PS chains into a PS homopolymer matrix, a system which has been well studied.⁴¹ For a matrix of high molecular weight homopolymer chains, interpenetration of end-tethered grafted chains occurs primarily via breathing mode relaxations of the grafted chains as they poke into the matrix.⁹⁷ Neutron reflectivity measurements by Clarke and Jones have characterized these timescales for various end-tethered and homopolymer chain lengths.^{98–100} For adsorbed chains comprised of tails, loops, and trains, we believe this analogy with end-grafted chains is reasonable for tails, but recognize that interpenetration of high molecular weight homopolymer chains with loops, especially tightly bound ones, would likely be a slower process and is still largely an open question.^{10,39} Neutron reflectivity measurements by Koga et al. have demonstrated that matrix PS chains can interpenetrate with “loosely adsorbed chains” (adsorbed layers comparable to those of the present study) with no significant evolution in the composition profile between 15 min and 24 h of annealing at 150 °C.⁵ However, more recent adhesion measurements primarily with poly(ethylene oxide) (PEO) found adhesion strength between matrix chains and an adsorbed layer to be poorly correlated with interpenetration determined from neutron reflectivity profiles, although good adhesion strength was reported for PS matrix chains annealed with loosely adsorbed chains at 170 °C ($T \gg T_g$).¹⁰

Case (iii) in Fig. 9 of a “regular” film corresponds to a sample that was only vacuum annealed overnight (13 h) at 120 °C, representing the most common sample preparation conditions used in the nanoconfinement literature. According to our data from Figure 8, when bulk films undergo this annealing condition and are then solvent washed with toluene, the resulting h_{ads} value is ≈ 1 nm. For a much thinner 31-nm thick film, we can estimate that

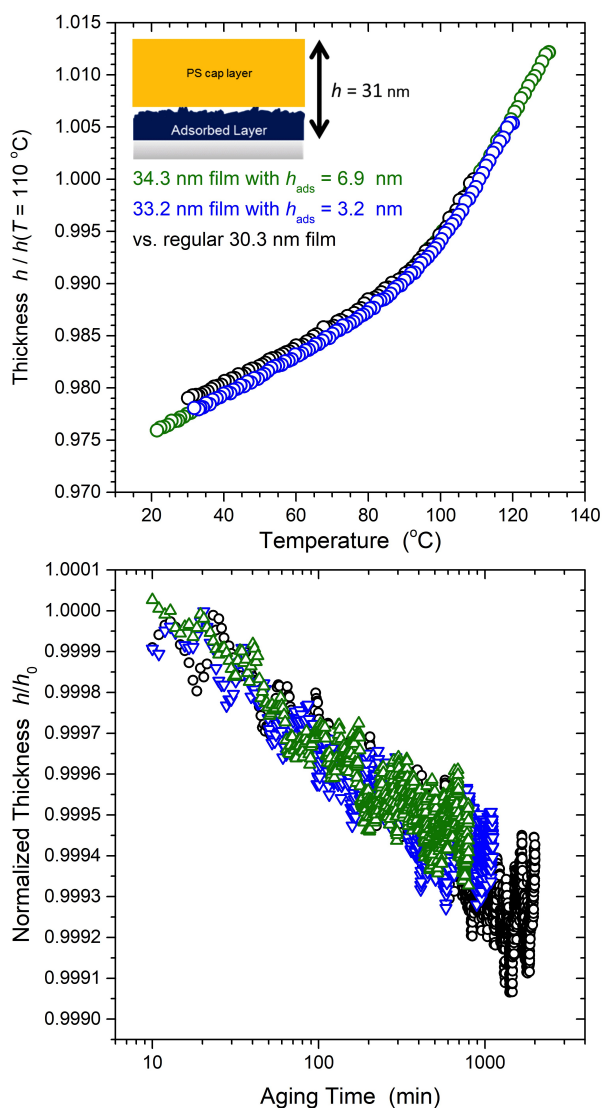


Fig. 9 Comparison of PS films made with explicit adsorbed layers of thickness h_{ads} preformed on the surface followed by floating a layer of thickness h_{float} atop and annealing to create films of total thickness $h_{\text{total}} = h_{\text{ads}} + h_{\text{float}} \approx 31$ nm. Green data have $h_{\text{ads}} = 6.9$ nm, blue data $h_{\text{ads}} = 3.2$ nm, while black data are for a regular 30.3 nm thick film simply spin-coated onto the silicon wafer. (Top) Graphs the film thickness, normalized at $T = 110$ °C, versus temperature used to determine the glass transition temperature $T_g = 93 \pm 1$ °C for all three samples. (Bottom) Graphs the film thickness, normalized at the start of the aging run $h_0(t_0 = 10$ min), as a function of aging time following a thermal quench from equilibrium above T_g to an aging temperature of 40 °C. Collapse of the data demonstrate no difference in the average glass transition and physical aging response for the three different kinds of samples.

such an annealed film would have a reduced h_{ads} value ≈ 0.5 nm after solvent washing based on the recent study by Napolitano et al.¹⁸ demonstrating that $h_{\text{ads}}(t)$ values are significantly reduced when the initial film thickness is decreased. Small h_{ads} values ≈ 0.5 nm are comparable to h_{ads} values obtained when simply washing off any film in solvent, including films that were never annealed as shown in Fig. 8. The physics behind polymer adsorption in solution implies that simply putting a clean substrate into a solution with some polymer chains will result in the chains coat-

ing the substrate and forming an adsorbed layer. Thus, it seems reasonable to consider this case (iii) condition of “regular” films to have $h_{\text{ads}} \approx 0$.

Figure 9 compares these three different samples with and without explicit h_{ads} layers, plotting the temperature-dependence of the film thickness $h(T)$, normalized to $h(T = 110$ °C), measured on cooling at 1 °C/min, and the normalized thickness h/h_0 as a function of aging time following a rapid (55 °C/min) quench to an aging temperature of 40 °C. The normalization condition h_0 represents the film thickness at an aging time of 10 min, following our previous works.^{74,76,82} All three samples show equivalent results, as can be visually seen in the figure by the superposition of the data. We note that multiple measurements on nominally identical samples typically show at least this much variation in the data.⁸² The average glass transition temperature $T_g(h)$ of the films were determined in the usual manner from the intersection of linear fits to the liquid and glassy regimes, giving an average of 93 ± 1 °C for all three samples. The physical aging rate characterizing the stability and densification of the glassy film as it evolves towards equilibrium is given by the slope of the data, and was measured to be on average $\beta = -d(h/h_0)/d(\log t) = 3.0 \pm 0.5 \times 10^{-4}$ for the three samples, equivalent to our previous works.^{76,82}

From these results, it appears that the presence or absence of an explicit adsorbed layer at the substrate interface does not affect the average glass transition temperature $T_g(h)$ and physical aging rate $\beta(h)$ of thin films. However, we recognize that *average* values may not fully represent *local* differences in dynamics near the interfaces. For example, the average $T_g(h)$ for PS films with PS chains end-grafted to the silica substrate have frequently shown little to no change in average $T_g(h)$ with the addition of the end-tethered chains.^{101–103} Yet, recent localized fluorescence measurements by Huang and Roth on samples designed to avoid competing free surface effects found that the local $T_g(z = 0)$ next to the silica substrate can increase by as much as +50 K with low grafting densities of only $\sigma = 0.011$ chains/nm².⁵¹ This apparent contradiction can be explained by the work of Lan and Torkelson¹⁰⁴ that chemically labeled pyrene dye to different locations of PS brushes, demonstrating that the local T_g of the brush near the substrate interface was strongly increased by +36 K while the local T_g near the free surface was strongly reduced by –14 K. These strong differences in *local* T_g at different positions within the film occurred despite measurements of the *average* $T_g(h)$ of the brush being predominantly unaltered from bulk, suggesting that local changes at the two interfaces largely canceled each other out. Thus, measurements of the local T_g next to adsorbed layers would be warranted.

The closest such local T_g measurements that already exist in the literature is that of Priestley et al. where adsorbed layers of pyrene-labeled PS were capped with unlabeled PS films, measuring the T_g of the adsorbed layer itself.²² They reported that depending on the initial annealing conditions used to create adsorbed layers of pyrene-labeled PS after three 10-min toluene washes, the local T_g of the adsorbed layer was found to be reduced from bulk when initially capped with the unlabeled PS layer, after a short anneal of only 20 min at 120 °C. Subsequent annealing at 150 °C of the stacked films to amalgamate the two

layers resulted in bulk T_g being recovered within a few hours. This time scale for slow interpenetration of the surface bound chains with an overlying polymer matrix is consistent with literature studies from the 1990s investigating the kinetics of end-grafted chains interpenetrating high molecular weight homopolymers.^{41,97–100} Adsorbed chains with some distribution of loops, tails, and trains could be expected to take even longer to achieve good interpenetration.^{10,39} Whereas tails can utilize relatively rapid breathing modes to penetrate into the overlying high molecular weight homopolymer,⁹⁷ loops would require the threading of the homopolymer chains, which could be a particularly slow process for small loops.³⁹ These results by Priestley et al.²² demonstrating that adsorbed chains recover bulk T_g with extended annealing conditions likely required to achieve good interpenetration of surface bound chains with the overlying PS matrix, suggest that perhaps adsorbed layers within a melt do not exhibit T_g perturbations.

4 Conclusions: Summary, Implications and Open Questions

We began our investigation into adsorbed layers in 2016 when trying to understand some unexpected results demonstrating a molecular weight dependence to the physical aging behavior of thin PS films.⁸² As the existing literature was proposing that chain adsorption in melt films may be altering dynamics in such thin films^{1–13} and that the adsorbed layer thickness measured increased with increasing molecular weight^{14,26,27} (as summarized in Fig. 1), we believed we should investigate and address the possibility that adsorbed layer formation may be responsible for the unexpected molecular weight dependent physical aging results we were observing in thin films. Our conclusions from this study⁸² were that we could find no experimental evidence to support the hypothesis that chain adsorption was responsible for our observed molecular weight dependent aging behavior. No variation in the annealing or preparation conditions that were reported to increase chain adsorption altered the observed physical aging behavior, nor the pre-formation of explicit adsorbed layers within a thin film as demonstrated in Fig. 9 of the present review.

During the course of that investigation, we needed to identify an appropriate experimental protocol for forming adsorbed layers from melt films via solvent washing and convince ourselves that we understood how to reliably form residual adsorbed layers of a given thickness h_{ads} . This review is a summary of our understanding from that process. In short, our main conclusion is that once the films have been immersed in solvent, the resulting system of chains adsorbed to a surface in solution is fundamentally equivalent to that used to grow adsorbed layers in solution, thus the same physics must apply.

4.1 Summary of Findings

Based on a survey of the disparate literature studies available at the time,^{4,14,22,26,27} we arrived at an experimental procedure most commonly used to form $h_{\text{ads}}(t)$ curves by solvent washing melt annealed films, where Figure 2 provides a summary of these steps. From our experimental efforts, we were forced to conclude

that the residual adsorbed layer thickness $h_{\text{ads}}(t)$ formed from this process, where h_{ads} is measured after a given solvent washing condition as a function of annealing time t of the film at an elevated temperature in the melt state prior to washing, are far less reproducible than implied in the literature. The largest source of variability we found corresponds to samples made in different batches, where a batch represents a group of silicon wafers all piranha cleaned together. The logistics and safety of piranha cleaning means that there are a finite number (≤ 15 samples) that can be made together in a single batch. By binning data together from different batches, as demonstrated in Figure 4, we were able to reproduce $h_{\text{ads}}(t)$ curves comparable to those from the literature (as shown in Fig. 1). $h_{\text{ads}}(t)$ data where the entire curve is collected from a single batch of samples, as in Fig. 7, appear to be the most like those reported in the literature.

From our investigation of forming $h_{\text{ads}}(t)$ curves by solvent washing melt annealed films, we found that the residual adsorbed layer thickness h_{ads} is almost entirely dependent on the solvent washing conditions used. In our efforts to understand this process, we consulted the extensive, well-established older literature on chain adsorption in solution, reviewing in Section 1.2 the understanding developed about chain adsorption that is pertinent to the interpretation of forming residual adsorbed layers by solvent washing melt films. We found there to be a disconnect in conceptual interpretation between the assumptions being made in the recent literature regarding producing adsorbed layers by solvent washing of melt films and this older literature on how adsorbed chains behave in solution that provides direct experimental evidence in contradiction to these assumptions. The recent literature believes that individual polymer segment–surface contacts are irreversibly adsorbed such that unadsorbed chains can be readily washed away from a film using a good solvent without disturbing the adsorbed chains and thereby “revealing” the structure of the adsorbed layer that is present within the film, a process which has come to be referred to as “Guiselin’s experiment”^{1,6,14–18} or “Guiselin’s approach”.^{10,19,20} This interpretation is based on a theoretical assumption by Guiselin³² that is experimentally invalid.

Numerous studies from the older literature demonstrate that adsorbed chains in solution are quite mobile and readily exchange with those in solution,^{34,37,38,59,61,62,64} with more recent experimental evidence directly demonstrating adsorbed chains crawl and hop across the surface, even in the limit of strong adsorption.^{54,67–69} Misunderstanding about the reversible/irreversible nature of adsorbed chains is long standing, with a 1987 review by de Gennes³⁵ laying out the arguments and experimental evidence for the reversibility of adsorbed chains despite the total equilibrium adsorbed amount Γ of a given layer being strongly conserved, simply giving the illusion of irreversible adsorption. In his review, de Gennes explicitly argued that the countervailing viewpoint in favor of irreversibility, which claims that all polymer segment–surface contacts need to be detached at once for a chain to desorb, is “utterly wrong”.³⁵ The correct picture that emerges from all the experimental evidence is that individual polymer segment–surface contacts are not irreversibly adsorbed, but readily detach and exchange with solvent or other polymer segments on

the same or different chain. With this continuous exchange of surface contacts, individual polymer chains can “unzip” from the surface and diffuse away.³⁵ Exchange experiments with a second “displacer” solvent also demonstrate reversibility with additional displacement of polymer chains observed when introducing a second solvent that has a more favorable interaction with the substrate,^{36,65,66} as defined by Silberberg’s adsorption energy parameter χ_s (eq. 3).⁵³ Such mobility of adsorbed chains in solution and these differences in χ_s with solvent likely explain recent reports by Koga et al.²⁰ and Beena Unni et al.⁷³ that residual h_{ads} adsorbed layers can end up dewetting in solution under some solvent conditions. Thus, the mobility of adsorbed polymer chains in solution means that the resulting residual adsorbed layer thickness h_{ads} remaining after solvent washing of films is primarily a representation of the solution conditions the films are washed in and likely bear little resemblance to any adsorbed state in the melt film. We find our experimental observations of the measured h_{ads} from solvent washing films to be consistent with this understanding from the older literature of polymer adsorption in solution.

We observe that part of the poor reproducibility of obtaining consistent $h_{\text{ads}}(t)$ values from following the experimental protocol outlined in Fig. 2 is that annealing at elevated temperatures above T_g is not required to form a perceived $h_{\text{ads}}(t)$ adsorbed layer. Simply having the films sit at room temperature for a few hours leads to densification of the films that make them harder to wash away, requiring longer exposure for the solvent to penetrate, swell, and dissolve the glassy film. Thus, for a given fixed solvent washing protocol, the remaining h_{ads} layer will be thicker giving the illusion of higher chain adsorption. This observation is consistent with the data shown by Koga et al.²⁶ that the long-time adsorbed layer thickness h_{∞} is independent of annealing temperature from 40-150 °C.

We also find that the substrate cleaning method strongly impacts the measured h_{ads} thickness, which is consistent with earlier work by Granick et al.⁹⁶ demonstrating that substrate cleaning treatment affects polymer adsorption in solution. As shown in Fig. 8, acid based cleaning methods like piranha and HCl solutions, typical of studies reporting adsorbed layer formation in melt films, consistently lead to larger h_{ads} values compared with simply rinsing the silicon wafer with an organic solvent like toluene. Tsui et al.²⁷ and Koga et al.²⁶ have demonstrated that HF cleaned silicon leads to even larger h_{ads} values than piranha cleaned silicon, as shown in Fig. 1b. For toluene cleaned silicon substrates, where the PS film was then annealed for 13 hours at only 120 °C, the sample preparation protocol most typical of studies in the nanoconfinement literature investigating property changes in thin films, the measured h_{ads} value is only ~ 1 nm, barely above the $h_{\text{ads}} \leq 0.24$ nm value we have concluded should be reasonably considered to be $h_{\text{ads}} \approx 0$ because it is impossible to distinguish from natural variations in the native oxide layer thickness.

To assess if the presence of an adsorbed layer h_{ads} could alter dynamics in thin films, we performed glass transition and physical aging measurements on samples with adsorbed chains. Given our observations that solvent washing does not provide a reliable

measure of the possible presence of an adsorbed layer in films, we created films with an explicit preformed adsorbed layer of known thickness h_{ads} . These known h_{ads} layers were then placed in ≈ 31 nm thick films by capping the h_{ads} layer with layers h_{float} to create $h_{\text{total}} = h_{\text{ads}} + h_{\text{float}} \approx 31$ nm. As shown in Figure 9, the average $T_g(h_{\text{total}} \approx 31$ nm) of these films did not vary for films with different h_{ads} thicknesses, including those with zero h_{ads} layer. The average physical aging rate $\beta(h_{\text{total}} \approx 31$ nm) at 40 °C also did not differ with or without the presence of different h_{ads} values.

From this investigation into chain adsorption, we conclude that the use of some protocol like that outlined in Figure 2 to measure an h_{ads} layer thickness is sufficiently irreproducible, and more reflective of the solvent washing conditions used to extract the layer, that to infer some role of chain adsorption in melt films from correlations of such $h_{\text{ads}}(t)$ values with measurements of dynamics on parallel samples seems questionable at best. It would also appear that the absence or presence of placing an explicit adsorbed layer within a thin film does not alter the measured average $T_g(h)$ and $\beta(h)$ dynamics.

4.2 Open Questions

During this process, we also identified a number of open question which we believe are worthy of further research:

- Just because the *average* film $T_g(h)$ and $\beta(h)$ dynamics do not change, does not necessarily imply that adsorbed chains are not imparting some *local* change in these properties. For example, Lan and Torkelson¹⁰⁴ recently demonstrated that PS brushes can have large gradients in local T_g with strongly elevated values near the substrate interface counteracted by reduced values near the free surface such that the average film $T_g(h)$ barely deviates from bulk despite this large gradient in local dynamics. Our group recently showed that low grafting density end-tethered chains can substantially increase the local $T_g(z)$ of the PS matrix near the substrate interface by as much as +50 K for only $\sigma = 0.011$ chains/nm².⁵¹ As adsorbed chains contain a mixture of loops, tails, and trains, it is not unrealistic to think that tails could be acting in a similar fashion to grafted end-tethered chains, and certainly the impact of loops bound to the surface is an open question. Thus, local measurements of the impact of adsorbed chains would be warranted and something our group is pursuing.
- An important open question related to the evaluation of whether adsorbed chains are locally impacting the dynamics of a polymer matrix is the temperature-dependent timescale needed for entanglement or interdiffusion of surface bound adsorbed chains with an overlying polymer matrix. Although tails could reasonably be interpreted in the context of end-tethered chains, for which much is known in this context,^{41,97-100} the entanglement of loops in particular may be entirely dependent on the homopolymer dynamics, which could be extremely long for high molecular weight chains. This was already identified as an open question in the context of adsorbed chains in polymer solution by Granick in 2002.³⁹ The experimental evaluation of the local impact of adsorbed chains in melts would likely involve the assembly of some type of $h_{\text{ads}} + h_{\text{float}}$ sample

with high molecular weight chains used to localize a fluorescent probe layer. Such long timescales needed for the interdiffusion of high molecular weight matrix chains with substrate bound chains to obtain sufficiently consolidated samples to remove the initially present free surface may explain the slow recovery of bulk T_g observed by Priestley et al.²² in their recent work. More recent work by Zuo et al. suggests that surface bound loops can modify dynamics in thin films, although the relative impact of small vs. large loops appears to be uncertain.^{6,105}

- The driving force for polymer adsorption in solution implies that simply inserting a clean substrate into a dilute polymer solution also results in a residual h_{ads} layer upon removal and drying of the substrate from solution.³⁴ These solution grown h_{ads} layers can be comparable in thickness to residual h_{ads} values obtained by solvent washing melt annealed films. Thus, a natural question would be to test whether there is any difference between these two types of adsorbed layers, especially given the significant polymer mobility of surface bound chains that occurs in solution.^{38,40,54,61,67–70} We have observed that films which were melt annealed at 150 °C for longer do result in thicker $h_{\text{ads}}(t)$ residual adsorbed layers after a given solvent washing condition. This suggests there is something different about these residual adsorbed layers that may reflect some slow evolution of substrate bound chains within the melt. However, as we have also observed that other factors which reduce film solubility, such as densification of the glassy film, also result in thicker $h_{\text{ads}}(t)$ residual adsorbed layers after a given solvent washing condition, it is possible that film annealing may simply reflect reduced film solubility requiring longer solvent washing times. This is also an open question we are pursuing in a subsequent publication.
- Theoretical efforts to understand polymer adsorption nearly all cite the same definition for the segmental “sticking” energy χ_s representing the favorable enthalpic polymer segment–surface interaction that drives adsorption, eq. 3. This original definition formulated by Silberberg⁵³ is based on the difference ($u_s - u_s^0$) in interaction energies between a polymer segment–surface contact u_s exchanging with a solvent–surface contact u_s^0 . However, as explained in Section 1.2, for a melt film with no solvent present, the relevant exchange of surface contacts would be between two equivalent polymer segment–surface contacts. As this would not have any enthalpic energy gain, χ_s would be strictly zero by the definition of eq. 3. Perhaps if there were some favorable (e.g., hydrogen bonding) interaction between the polymer and substrate surface, there could be an enthalpic energy barrier that would need to be overcome for the exchange of polymer segment–surface contacts. This could conceivably be defined in terms of the difference in interaction energies between a polymer segment–surface contact and a polymer segment–segment contact in the bulk, but a different theoretical framework would be needed for this as this would not be equivalent to eq. 3. The other main factor driving adsorption in solution is the reduced miscibility of large chains in solution,³⁴ which is also not present in a melt film. Thus, it is not clear whether chain adsorption even occurs within melt

films.

- Consistent with recent literature reports,^{4,14,15,22,26,27} we do observe that the residual $h_{\text{ads}}(t)$ thickness increases with increasing annealing time, where t represents the length of time the PS films were held in their melt state at 150 °C prior to being washed with some given solvent procedure. This is indicative of the films being harder to wash off. From an examination of our $h_{\text{ads}}(t)$ data in Figures 4, 5, 7, and 8, we do find some evidence suggesting that a slow restructuring of chain conformations near the substrate interface may be occurring within the melt films during this extended annealing at 150 °C. However, as any substrate bound chains will have considerable mobility and change conformation as soon as they are exposed to solvent, we believe inferring such information from any $h_{\text{ads}}(t)$ data after solvent washing provides limited insight. There are some literature studies that have tried to measure in-situ the dynamics of surface bound chains within the melt as a function of different annealing conditions,^{2,9,22,88,106} but frequently these measurements still involve interpretation where $h_{\text{ads}}(t)$ data or literature reports thereof are used to attribute the changes to increased adsorption in the melt. There are also tracer diffusion studies reporting reduced mobility of chains near a substrate interface. Early work from the mid-1990s by Rafailovich et al. reported reduced diffusion from bulk of PS chains by up to 3 orders of magnitude near a SiOx/Si interface, scaling as $D_{\text{surf}} \sim N^{-1.5}$.⁸⁶ In collaboration with Rubinstein, this was interpreted at the time as a “stickiness” of the interface where polymer segment–surface contacts increased the friction coefficient for reptation, where $N^{1/2}$ surface contacts per chain for Gaussian conformations gave the correct scaling. However, reduced diffusion by an order of magnitude persisted for an extended distance of ≈ 100 nm away from the interface indicating that direct surface contacts were not required.⁸⁷ Split layer experiments suggested that entanglements with matrix chains that can span to the substrate interface were required to slow diffusion. At this point, all we can conclude is that this is still a major open question, with several results indicating that dynamics are slower near a substrate interface in the melt, although not all measurements are straightforward to interpret. It is unclear if the system is meaningfully evolving to some equilibrium state, which may or may not be different than the chain conformations of surface bound chains obtained in theta-solvent conditions, or if the dynamics are simply so slow that only non-equilibrium conformations are obtained.¹⁰⁷
- Finally, given the commonalities between polymer–interface interactions in films and polymer nanocomposites (PNCs), a better understanding of chain adsorption in melts has broader implications than only in the film studies cited so far. Studies of PNCs frequently interpret the impact of nanofiller interfacial interactions on the polymer matrix based on the presence of a “bound layer” at the surface of nanoparticles (NPs).^{108–110} In fact, a widespread procedure for determining the thickness δ of this bound layer is very similar to the Figure 2 procedure. A good solvent is used to dissolve away any unbound matrix chains, after which thermogravimetric analysis (TGA) is used to determine the remaining “bound” polymer to NP fraction,

with δ calculated assuming a spherical shell of polymer with bulk density around the NP.¹⁰⁹ Other common themes between films and PNCs include, the requirement for good interpenetration between surface bound and matrix chains to cause observable changes in dynamics,^{95,110,111} as well as the reduced mobility of these surface bound chains. For PNC studies on P2VP/SiO₂-NPs where attractive hydrogen bonding interactions are present, reduced τ_{α} relaxation times of surface bound chains by two orders of magnitude have been reported.¹¹² However, even in these strongly bonded systems, the surface bound chains are not irreversibly adsorbed, but can exchange with matrix chains.⁸⁹ The strong temperature dependence observed for this exchange lifetime is consistent with reports from solution studies where surface coverage is shown to be reduced at higher temperatures when more thermal energy is available to overcome the predominantly temperature-independent binding energy of the surface bound chains.⁵⁴ Given these similarities, there may be much that can be learned from making connections to the previously developed understanding about polymer adsorption in solution.

Conflicts of interest

The authors declare no competing financial interest.

Acknowledgements

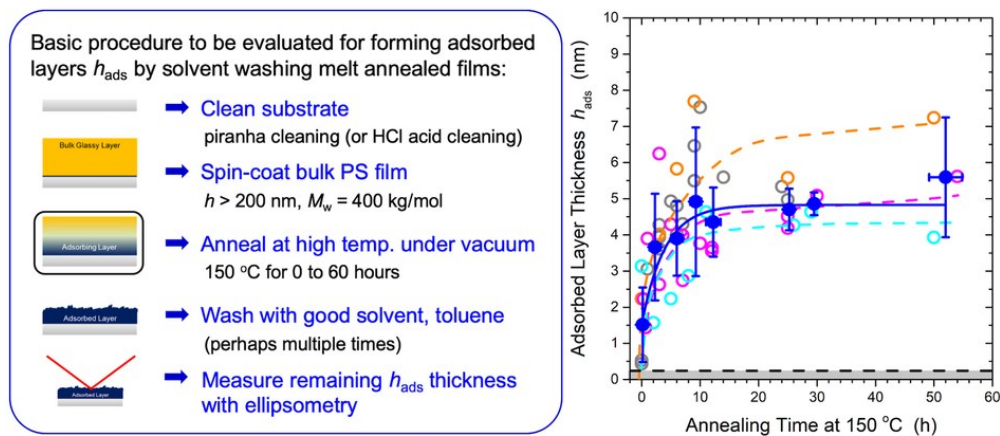
The authors gratefully acknowledge support from the National Science Foundation Polymers Program (DMR-1709132 and DMR-1905782) and Emory University.

References

- 1 S. Napolitano and M. Wubbenhorst, *Nature Communications*, 2011, **2**, 260.
- 2 T. Koga, N. Jiang, P. Gin, M. K. Endoh, S. Narayanan, L. B. Lurio and S. K. Sinha, *Physical Review Letters*, 2011, **107**, 225901.
- 3 S. Napolitano, S. Capponi and B. Vanroy, *European Physical Journal E*, 2013, **36**, 61.
- 4 N. Jiang, J. Shang, X. Di, M. K. Endoh and T. Koga, *Macromolecules*, 2014, **47**, 2682 – 2689.
- 5 N. Jiang, J. Wang, X. Di, J. Cheung, W. Zeng, M. K. Endoh, T. Koga and S. K. Satija, *Soft Matter*, 2016, **12**, 1801 – 1809.
- 6 S. Sun, H. Xu, J. Han, Y. Zhu, B. Zuo, X. Wang and W. Zhang, *Soft Matter*, 2016, **12**, 8348 – 8358.
- 7 A. Panagopoulou and S. Napolitano, *Physical Review Letters*, 2017, **119**, 097801.
- 8 N. G. Perez-de Eulate, M. Sferrazza, D. Cangialosi and S. Napolitano, *ACS Macro Letters*, 2017, **6**, 354 – 358.
- 9 Y. Zhou, Q. He, F. Zhang, F. Yang, S. Narayanan, G. Yuan, A. Dhinojwala and M. D. Foster, *ACS Macro Letters*, 2017, **6**, 915 – 919.
- 10 N. Jiang, M. Sen, W. Zeng, Z. Chen, J. M. Cheung, Y. Morimitsu, M. K. Endoh, T. Koga, M. Fukuto, G. Yuan, S. K. Satija, J.-M. Y. Carrillo and B. G. Sumpter, *Soft Matter*, 2018, **14**, 1108 – 1119.
- 11 N. Jiang, M. Sen, M. K. Endoh, T. Koga, E. Langhammer, P. Björn and M. Tsige, *Langmuir*, 2018, **34**, 4199 – 4209.
- 12 A. Debot, P. Tripathi and S. Napolitano, *European Physical Journal E*, 2019, **42**, 102.
- 13 X. Li and X. Lu, *ACS Macro Letters*, 2019, **8**, 1426 – 1431.
- 14 C. Housmans, M. Sferrazza and S. Napolitano, *Macromolecules*, 2014, **47**, 3390 – 3393.
- 15 D. N. Simavilla, A. Panagopoulou and S. Napolitano, *Macromolecular Chemistry And Physics*, 2018, **219**, 1700303.
- 16 M.-L. Braatz, L. I. Meléndez, M. Sferrazza and S. Napolitano, *Journal of Chemical Physics*, 2017, **146**, 203304.
- 17 D. N. Simavilla, W. Huang, P. Vandestrack, J.-P. Ryckaert, M. Sferrazza and S. Napolitano, *ACS Macro Letters*, 2017, **6**, 975 – 979.
- 18 D. N. Simavilla, W. Huang, C. Housmans, M. Sferrazza and S. Napolitano, *ACS Central Science*, 2018, **4**, 755 – 759.
- 19 M. Sen, N. Jiang, J. Cheung, M. K. Endoh, T. Koga, D. Kawaguchi and K. Tanaka, *ACS Macro Letters*, 2016, **5**, 504 – 508.
- 20 N. Jiang, J. Cheung, Y. Guo, M. K. Endoh, T. Koga, G. Yuan and S. K. Satija, *Macromolecular Chemistry And Physics*, 2018, **219**, 1700326.
- 21 S. Napolitano and D. Cangialosi, *Macromolecules*, 2013, **46**, 8051 – 8053.
- 22 M. J. Burroughs, S. Napolitano, D. Cangialosi and R. D. Priestley, *Macromolecules*, 2016, **49**, 4647 – 4655.
- 23 A. B. Unni, G. Vignaud, J. P. Chapel, J. Giermanska, J. K. Bal, N. Delorme, T. Beuvier, S. Thomas, Y. Grohens and A. Gibaud, *Macromolecules*, 2017, **50**, 1027 – 1036.
- 24 H. Jeong, S. Napolitano, C. B. Arnold and R. D. Priestley, *Journal of Physical Chemistry Letters*, 2017, **8**, 229 – 234.
- 25 H. K. Nguyen, M. Labardi, M. Lucchesi, P. Rolla and D. Prevosto, *Macromolecules*, 2013, **46**, 555 – 561.
- 26 P. Gin, N. Jiang, C. Liang, T. Taniguchi, B. Akgun, S. K. Satija, M. K. Endoh and T. Koga, *Physical Review Letters*, 2012, **109**, 265501.
- 27 Y. Fujii, Z. Yang, J. Leach, H. Atarashi, K. Tanaka and O. K. C. Tsui, *Macromolecules*, 2009, **42**, 7418 – 7422.
- 28 X. Huang and C. B. Roth, *Journal of Chemical Physics*, 2016, **144**, 234903.
- 29 H. Fujiwara, *Spectroscopic Ellipsometry: Principles and Applications*, John Wiley & Sons, Ltd., West Sussex, England, 2007.
- 30 S. Napolitano and M. Sferrazza, *Advances In Colloid And Interface Science*, 2017, **247**, 172 – 177.
- 31 C. J. Durning, B. O'Shaughnessy, U. Sawhney, D. Nguyen, J. Majewski and G. S. Smith, *Macromolecules*, 1999, **32**, 6772 – 6781.
- 32 O. Guiselin, *Europhysics Letters*, 1992, **17**, 225 – 230.
- 33 E. Jenckel and B. Rumbach, *Zeitschrift für Elektrochemie und angewandte physikalische Chemie*, 1951, **55**, 612 – 618.
- 34 G. J. Fleer, M. A. Cohen Stuart, J. M. H. M. Scheutjens, T. Cosgrove and B. Vincent, *Polymers at Interfaces*, Chapman & Hall, London, UK, 1993.

- 35 P. G. d. de Gennes, *Advances In Colloid And Interface Science*, 1987, **27**, 189 – 209.
- 36 M. A. C. Stuart, G. J. Fleer and J. M. H. M. Scheutjens, *Journal of Colloid And Interface Science*, 1984, **97**, 515 – 525.
- 37 M. A. Cohen Stuart and G. J. Fleer, *Annual Review of Materials Science*, 1996, **26**, 463 – 500.
- 38 S. Granick, *Physics of Polymer Surfaces and Interfaces*, I. C. Sanchez, Ed.; Butterworth-Heinemann, Boston, 1992, ch. 10: Dynamics of Adsorption and Desorption at Polymer/Solid Interfaces, pp. 227–244.
- 39 S. Granick, *European Physical Journal E*, 2002, **9**, 421 – 424.
- 40 J. F. Douglas, H. M. Schneider, P. Frantz, R. Lipman and S. Granick, *Journal of Physics-Condensed Matter*, 1997, **9**, 7699 – 7718.
- 41 R. A. L. Jones and R. W. Richards, *Polymers at Surfaces and Interfaces*, Cambridge University Press, Cambridge, UK, 1999.
- 42 W. Norde, *Advances In Colloid And Interface Science*, 1986, **25**, 267 – 340.
- 43 R. R. Netz and D. Andelman, *Physics Reports*, 2003, **380**, 1 – 95.
- 44 H.-J. Butt, K. Graft and M. Kappl, *Physics and Chemistry of Interfaces*, Wiley-VCH Verlag GmbH, Weinheim, Germany, 2013.
- 45 A. W. Adamson and A. P. Gast, *Physical Chemistry of Surfaces*, 6th Edition, Wiley, New York, 1997.
- 46 H. Swenson and N. P. Stadie, *Langmuir*, 2019, **35**, 5409–5426.
- 47 J. M. H. M. Scheutjens and G. J. Fleer, *J Phys Chem*, 1979, **83**, 1619 – 1635.
- 48 J. M. H. M. Scheutjens and G. J. Fleer, *J Phys Chem*, 1980, **84**, 178 – 190.
- 49 P. G. d. Gennes, *Journal de Physique*, 1976, **37**, 1445 – 1452.
- 50 M. Aubouy, O. Guiselin and E. Raphael, *Macromolecules*, 1996, **29**, 7261 – 7268.
- 51 X. Huang and C. B. Roth, *ACS Macro Letters*, 2018, **7**, 269 – 274.
- 52 T. Wang, J. Yan, H. Yuan, J. Xu, H. Y. Lam, X. Yu, C. Lv, B. Du and O. K. C. Tsui, *ACS Macro Letters*, 2019, **8**, 1280 – 1284.
- 53 A. Silberberg, *J Phys Chem*, 1962, **66**, 1872 – 1883.
- 54 C. Yu and S. Granick, *Langmuir*, 2014, **30**, 14538 – 14544.
- 55 H. M. Schneider and S. Granick, *Macromolecules*, 1992, **25**, 5054 – 5059.
- 56 M. Rubinstein and R. H. Colby, *Polymer Physics*, Oxford University Press, Oxford; New York, 2003.
- 57 H. M. Schneider, P. Frantz and S. Granick, *Langmuir*, 1996, **12**, 994 – 996.
- 58 M. M. Santore, *Current Opinion In Colloid & Interface Science*, 2005, **10**, 176 – 183.
- 59 E. Pefferkorn, A. Haouam and R. Varoqui, *Macromolecules*, 1989, **22**, 2677 – 2682.
- 60 P. Frantz and S. Granick, *Physical Review Letters*, 1991, **66**, 899 – 902.
- 61 H. E. Johnson and S. Granick, *Macromolecules*, 1990, **23**, 3367 – 3374.
- 62 J. F. Douglas, H. E. Johnson and S. Granick, *Science*, 1993, **262**, 2010 – 2012.
- 63 H. E. Johnson, J. F. Douglas and S. Granick, *Physical Review Letters*, 1993, **70**, 3267 – 3270.
- 64 E. Pefferkorn, A. Carroy and R. Varoqui, *Journal of Polymer Science: Polymer Physics Edition*, 1985, **23**, 1997 – 2008.
- 65 G. P. van der Beek, M. A. Cohen Stuart, G. J. Fleer and J. E. Hofman, *Langmuir*, 1989, **5**, 1180 – 1186.
- 66 G. P. van der Beek, M. A. Cohen Stuart, G. J. Fleer and J. E. Hofman, *Macromolecules*, 1991, **24**, 6600 – 6611.
- 67 J. Zhao and S. Granick, *Macromolecules*, 2007, **40**, 1243 – 1247.
- 68 C. Yu, J. Guan, K. Chen, S. C. Bae and S. Granick, *ACS Nano*, 2013, **7**, 9735 – 9742.
- 69 K. H. Nagamanasa, H. Wang and S. Granick, *Advanced Materials*, 2017, **29**, 1703555.
- 70 M. J. Skaug, J. Mabry and D. K. Schwartz, *Physical Review Letters*, 2013, **110**, 256101.
- 71 H. G. Tompkins, *A User's Guide to Ellipsometry*, Academic Press, Inc., San Diego, CA, 1993.
- 72 S. Napolitano, C. Rotella and M. Wubbenhorst, *ACS Macro Letters*, 2012, **1**, 1189 – 1193.
- 73 A. Beena Unni, G. Vignaud, J. K. Bal, N. Delorme, T. Beuvier, S. Thomas, Y. Grohens and A. Gibaud, *Macromolecules*, 2016, **49**, 1807 – 1815.
- 74 E. A. Baker, P. Rittigstein, J. M. Torkelson and C. B. Roth, *Journal of Polymer Science Part B-Polymer Physics*, 2009, **47**, 2509 – 2519.
- 75 C. M. Herzinger, B. Johs, W. A. McGahan, J. A. Woollam and W. Paulson, *Journal of Applied Physics*, 1998, **83**, 3323 – 3336.
- 76 J. E. Pye, K. A. Rohald, E. A. Baker and C. B. Roth, *Macromolecules*, 2010, **43**, 8296 – 8303.
- 77 N. L. Thomas and A. H. Windle, *Polymer*, 1982, **23**, 529–542.
- 78 J. S. Papanu, D. W. Hess, A. T. Bell and D. S. Soane, *Journal of the Electrochemical Society*, 1989, **136**, 1195 – 1200.
- 79 J. S. Papanu, D. W. Hess, D. S. Soane and A. T. Bell, *Journal of the Electrochemical Society*, 1989, **136**, 3077–3083.
- 80 H. Coll and C. Searles, *Polymer*, 1988, **29**, 1266–1272.
- 81 D. Meng, K. Zhang and S. K. Kumar, *Soft Matter*, 2018, **14**, 4226 – 4230.
- 82 M. F. Thees and C. B. Roth, *Journal of Polymer Science Part B-Polymer Physics*, 2019, **57**, 1224–1238.
- 83 H. Richardson, I. Lopez-Garcia, M. Sferrazza and J. L. Keddie, *Physical Review E*, 2004, **70**, 051805.
- 84 H. Richardson, M. Sferrazza and J. L. Keddie, *European Physical Journal E*, 2003, **12**, S87 – S91.
- 85 J. M. Hutchinson, *Progress In Polymer Science*, 1995, **20**, 703 – 760.
- 86 X. Zheng, B. B. Sauer, J. G. Vanalsten, S. A. Schwarz, M. H. Rafailovich, J. Sokolov and M. Rubinstein, *Physical Review Letters*, 1995, **74**, 407 – 410.

- 87 X. Zheng, M. H. Rafailovich, J. Sokolov, Y. Strzhemechny, S. A. Schwarz, B. B. Sauer and M. Rubinstein, *Physical Review Letters*, 1997, **79**, 241 – 244.
- 88 J. Choi, N. Clarke, K. I. Winey and R. J. Composto, *Macromolecules*, 2017, **50**, 3038 – 3042.
- 89 A. M. Jimenez, D. Zhao, K. Misquitta, J. Jestin and S. K. Kumar, *ACS Macro Letters*, 2019, **8**, 166 – 171.
- 90 F. Chen, K. Takatsuji, D. Zhao, X. Yu, S. K. Kumar and O. K. C. Tsui, *Soft Matter*, 2017, **13**, 5341 – 5354.
- 91 S. Alexander, *Journal de Physique*, 1977, **38**, 983 – 987.
- 92 P. G. de Gennes, *Macromolecules*, 1980, **13**, 1069 – 1075.
- 93 A. Casoli, M. Brendlé, J. Schultz, P. Auroy and G. Reiter, *Langmuir*, 2001, **17**, 388 – 398.
- 94 B. O'Shaughnessy and D. Vavylonis, *Journal of Physics-Condensed Matter*, 2005, **17**, R63 – R99.
- 95 A. P. Holt, V. Bocharova, S. Cheng, A. M. Kisliuk, B. T. White, T. Saito, D. Uhrig, J. P. Mahalik, R. Kumar, A. E. Imel, T. Etampawala, H. Martin, N. Sikes, B. G. Sumpter, M. D. Dadmun and A. P. Sokolov, *ACS Nano*, 2016, **10**, 6843 – 6852.
- 96 P. Frantz and S. Granick, *Langmuir*, 1992, **8**, 1176 – 1182.
- 97 K. P. O'Connor and T. C. B. McLeish, *Macromolecules*, 1993, **26**, 7322 – 7325.
- 98 C. J. Clarke, *Polymer*, 1996, **37**, 4747 – 4752.
- 99 C. J. Clarke, R. A. L. Jones and A. S. Clough, *Polymer*, 1996, **37**, 3813 – 3817.
- 100 C. J. Clarke, R. A. L. Jones, J. L. Edwards, K. R. Shull and J. Penfold, *Macromolecules*, 1995, **28**, 2042 – 2049.
- 101 M. Hénot, A. Chenneviere, E. Drockenmuller, K. Shull, L. Léger and F. Restagno, *European Physical Journal E*, 2017, **40**, 11.
- 102 J. L. Keddie and R. A. L. Jones, *Israel Journal of Chemistry*, 1995, **35**, 21 – 26.
- 103 A. Clough, D. Peng, Z. Yang and O. K. C. Tsui, *Macromolecules*, 2011, **44**, 1649 – 1653.
- 104 T. Lan and J. M. Torkelson, *Polymer*, 2015, **64**, 183 – 192.
- 105 B. Zuo, H. Zhou, M. J. B. Davis, X. Wang and R. D. Priestley, *Physical Review Letters*, 2019, **122**, 217801.
- 106 H. K. Nguyen, S. Sugimoto, A. Konomi, M. Inutsuka, D. Kawaguchi and K. Tanaka, *ACS Macro Letters*, 2019, **8**, 1006 – 1011.
- 107 S. Chandran, J. Baschnagel, D. Cangialosi, K. Fukao, E. Glynos, L. M. C. Janssen, M. Müller, M. Muthukumar, U. Steiner, J. Xu, S. Napolitano and G. Reiter, *Macromolecules*, 2019, **52**, 7146–7156.
- 108 S. K. Kumar, V. Ganesan and R. A. Riggleman, *Journal of Chemical Physics*, 2017, **147**, 020901.
- 109 N. Jouault, J. F. Moll, D. Meng, K. Windsor, S. Ramcharan, C. Kearney and S. K. Kumar, *ACS Macro Letters*, 2013, **2**, 371 – 374.
- 110 F. W. Starr, J. F. Douglas, D. Meng and S. K. Kumar, *ACS Nano*, 2016, **10**, 10960 – 10965.
- 111 W. Zhang, J. F. Douglas and F. W. Starr, *Journal of Chemical Physics*, 2017, **147**, 044901.
- 112 A. P. Holt, P. J. Griffin, V. Bocharova, A. L. Agapov, A. E. Imel, M. D. Dadmun, J. R. Sangoro and A. P. Sokolov, *Macromolecules*, 2014, **47**, 1837 – 1843.



79x39mm (300 x 300 DPI)